Design and Analysis of a Novel Renewable Multi-Generation System through Energetic and Exergetic Investigation

Nima Khosravi

Submitted to the
Institute of Graduate Studies and Research
in partial fulfillment of the requirements for the degree of

Master of Science
in
Mechanical Engineering

Eastern Mediterranean University
February 2017
Gazimağusa, North Cyprus

Approval of the Institute of Graduate Studies and Research

_____
Prof. Dr. Mustafa Tümer
Director

I certify that this thesis satisfies the requirements as a thesis for the degree of Master of Science in Mechanical Engineering.

_____
Assoc. Prof. Dr. Hasan Hacişevki
Chair, Department of Mechanical Engineering

We certify that we have read this thesis and that in our opinion it is fully adequate in scope and quality as a thesis for the degree of Master of Science in Mechanical Engineering.

_____
Dr. Devrim Aydın
Supervisor

Examining Committee
_____

1. Assoc. Prof. Dr. Hasan Hacişevki   _____

2. Asst. Prof. Dr. Neriman Özada   _____

3. Dr. Devrim Aydın   _____

ABSTRACT

There are many studies and research conducted on the multi-generation systems, however there is still a gap for some contributions. By reviewing the literature in the renewable source of energy it is explicit that many researchers performed number of studies about the design and analysis of multi-generation systems. However, none of them have chosen n-pentane for fluid running in an Organic Rankine Cycle (ORC), neither the thermal assessment of the multi-generation system have been studied. The primary goal of this research is to layout a novel multi-generation utility based on geothermal energy driven ORC, which is used to generate domestic electricity, heating, cooling and drying. Generated electricity can be partially used for domestic needs while the rest is proposed to utilize the hydrogen generated by electrolyte. The heat recovery of the ORC cycle drive a single effect absorption chiller (SEAC) for producing heating, cooling and dry air. Thereby, it is aimed to demonstrate an efficient process with improved energetic and exergetic efficiency. In this study the mass flow rate of the geothermal is 11.88 kg/s and the origin temperature is 483.2 K while utility energetic and exergetic efficiencies are 1.537 and 0.4121 respectively.

Keyword: multi-generation systems, exergetic assessment, geothermal

ÖZ

Çoklu üretim sistemleri üzerinde çeşitli çalışmalar gerçekleştirilmiş olmasına ragmen, bu sistemlerin hala gelişime açık yönleri mevcuttur. Yenilenebilir enerji kaynakları alanında yapılan literatür taraması sonucunda, birçok araştırmacının çoklu üretim sistemlerinin tasarımı ve analizi konularında çeşitli çalışmalar yaptıkları bulgusuna ulaşılmıştır. Ancak, bir çoklu üretim sistemi olan Organik Rankine Çevrimi (ORÇ) alanında yapılan literatur incelemesinde, n-pentane'ın çalışma akışkanı olarak seçildiği bir çalışma bulunamamıştır. Bunun yanında, bu çalışma akışkanını kullanan çoklu üretim sistemlerinin ısıl analizi alanında da herhangi bir çalışmaya rastlanmamıştır. Bu projenin temel amacı konutlarda elektrik üretimi, ısıtma, soğutma ve kurutma amaçlı kullanılabilecek, jeotermal enerji kaynaklı bir Organik Rankine Çevrimi tasarlamaktır. Çevrimde üretilecek elektriğin bir bölümünün konutlarda direk kullanımı, bir bölümünün ise elektrolit vasıtası ile hidrojen üretimi amaçlı kullanımı öngörülmüştür. Bunun yanında, çevrimde atık ısısının geri kazanılarak, absorbsiyonlu ısı pompası ünitesinin tahrik edilmesi ve bu yolla ısıtma, soğutma ve kurutma eldesi amaçlanmıştır. Tasarlanan çoklu üretim sisteminde, atık ısı geri kazanılarak sistemden faydalanabirliğin ve sistem performansının arttırılması, böylece enerji ve ekserji verimliliği yüksek bir proses geliştirilmesi hedeflenmiştir. Çalışma sonucuna göre, debisi 11.88 kg/s ve sıcaklığı 483.2 K olan jeotermal kaynağın kullanıldığı çoklu üretim sisteminin enerji ve ekserji verimliliği sırasıyla 1.537 ve 0.4121 olarak bulunmuştur.

Anahtar kelimeler: çoklu üretim sistemleri, ekserji analizi, jeotermal

ACKNOWLEDGMENT

I would like to express my sincere gratitude to my advisor Dr. Devrim Aydın for the continuous support of my Master thesis and related research, for his patience, motivation, and immense knowledge. His guidance helped me in all the time of research and writing of this thesis. I could not have imagined having a better advisor and mentor for my study.

My sincere thanks also goes to Assist. Prof. Dr. Neriman Özada, because of her very valuable comments on this thesis. Without her precious support it would not be possible to conduct this research

TABLE OF CONTENTS

LIST OF TABLES

LIST OF FIGURES

LIST OF ABBREVIATIONS

ṁ	Mass Flow Rate (kg/s)
v	Specific Volume (m^3/kg)
p	Pressure (kPa)
h	Enthalpy (kJ/kg)
T	Temperature (°C, K)
W	Work (kW)
$\dot{Q}$	Heat Flow Rate (kW)
HHV	High Heating Value (kJ/kg)
Ex	Exergy (kW)
$\dot{Ex}_d$	Exergy destruction rate (kW)
En	Energy (kW)
Ex_{ph}	Physical Exergy (kW)
Ex_{ch}	Chemical Exergy (kW)
MW	Molar Mass (kg/mol)
COP	Coefficient of Performance
η	Efficiency

Subscripts

Abs	Absorber
Cond	Condenser
Evap	Evaporator
Hx	Heat Exchanger
Geo	Geothermal
Turb	Turbine

d	Destruction
X	Concentration of the Solution
H_2	Hydrogen
avg	Average
1,..,23	State Numbers
0	Ambient

Acronyms

SEAC	Single Effect Absorption Chiller
ORC	Organic Rankine Cycle
EES	Engineering Equation Solver
WEC	World Energy Council
PEM	Proton Exchange Membrane
AHW	Atomic Hydrogen Welding
CFC	Chlorofluorocarbon

Chapter 1

INTRODUCTION

1.1 Background

One of the preliminary factors in the progression of a country is energy. As the population in the world increase, the energy demand raised up gradually. But the sources of fossil fuels are limited, and because of this problem investigation for finding an alternative source of energy such as renewable energy precipitated, that can eliminate energy conflicts. The use of natural sources of energy limited by quality, the density of production and validity. For reduction of global warming, many modern technologies have designed and tested. Global warming is a menace for today world because it shows that the average of the temperature of the environment has increased rapidly and by using various methods should detract this problem. As the efficiency, operation and maintenance cost, as well as pollution emissions of multi-generation systems, are significant it can act as major part in the energy field. Innumerable sources of renewable energy are available such as wind, biomass, Ocean thermal, Ocean current and geothermal. Geothermal energy is a sustainable and secure source of energy that can be applicable coupled with Organic Rankine Cycle (ORC) and single effect absorption chiller (SEAC) to produce multiple outcomes like electricity, cooling, heating, and drying.

1.2 Renewable energy

Origins of renewable energy are those supplies which can be exerted to generate energy many times, like solar power, wind power, geothermal energy, etc. (Panwar, 2007). Nowadays renewable technologies are one of the cleanest sources of energy which reduce the impact on the environment and produce wastes at a minimum level. Furthermore, these are sustainable according to current and future needs of people. By using the technologies of renewable energy, it is possible to diminish global warming and emission of greenhouse gas rather than conventional types of energy. Renewable energy sources (RES) extend nearly 15% of the overall request of energy in the world (Goldemberg, 2000). As the price of gas and oil is altering and the cost of RES reducing consistently, the passage of RES accelerated. By progression and installation of the project of renewable energy in the countryside, it is possible to increase the job opportunities and income of families.

1.3 Multi-generation system

As the population in the world grew rapidly, the demand for energy has raised up dramatically which leads to finding new technologies to produce energy with the minimum use of fossil fuels and consequently eliminate emissions produced by them, so various systems and modern technologies developed to reduce the greenhouse effect. One of them is the multi-generation system because it has high efficiency with minimum pollution emission. Moreover, the operating cost of it is negligible compared to rest. In multi-generation energy systems, it is conceivable to get multifold outputs from one or more energy sources. The final goal of using such a system is to gain efficiency and decline the cost of production and maintenance and also environmental side effects. This system can produce various outputs like electricity, heating, cooling, drying, and hydrogen.

In this system, both organic Rankine cycle and single effect absorption chiller are coupled together to produce required outputs. The organic Rankine cycle can take the energy needed from geothermal source and generate electricity and hydrogen. Furthermore, SEAC can turn out the cooling, heating and dry air.

1.4 Advantages of Multi-generation systems

Minimum waste, greenhouse effect and loss of thermal energy, better exergy and energy efficiency, minor operating cost and significant use of various resources are some of the preponderances of multi-generation systems (I Dincer & Zamfirescu, 2012). In such systems, the energy efficiency of the facility can rise by injecting the heat loss and waste energy of some parameters back into system consequently the overall performance of cycle will increase.

1.5 Aims and Objectives

The principal concern of this project is to design and analysis the energy and exergy of a novel multi-generation system based on ORC and SEAC by engineering equation solver (EES). By writing the various equations on the thermodynamic assessment of the utility in this software, it is possible to get a detailed output on the performed design. One of the purposes is to analyze the cycle performance and the COP of it moreover obtaining the efficiency of the subsystems. The destruction exergy is another term which is studied.

By reviewing the literature in the renewable source of energy, it is explicit that many kinds of research have been carried out on multi-generation systems. However, there is room for improvement of the overall performance of the individual systems and overall multi-generation system by using heat recovery. Moreover, none of them have chosen n-pentane as a working fluid in an (ORC), neither the energy and exergy analysis of the multi-generation system based on this fluid have studied. This study

performed to shows more efficient methods for producing various outputs for indoor applications.

The objectives of this study listed as below:

- Review of previous researches in the field

- Design a multi-generation system that uses geothermal energy and generate electricity, hydrogen, heating, cooling and dry air

- Developing energetic and exergetic analysis model

- Investigating the overall thermal performance of the system

This task categorized into five chapters. Chapter one introduces the background of the renewable energy and multi-generation system. Chapter two is the literature and history of this scheme. The description of the cycle presented in chapter three. The results and analysis of this plan rendered in chapter four. The last chapter which is number five is the conclusion.

Chapter 2

LITERATURE REVIEW ON MULTI-GENERATION SYSTEM

2.1 Background

In the present chapter, an exhaustive study of multi-generation systems and renewable energy demonstrated. Due to economic aspect's and environmental influence of exploiting fossil fuels to produce the energy inclination for exploiting the renewable energy sources like, multi-generation systems raised up rapidly. The primary purpose of this system is to enhance the exergy and energy performance of the utility while diminishing the side efficacy on the environment. In this study, the utility gains its energy from the geothermal source provided ORC together with SEAC produces the outputs. This utility provides heating, cooling, hot water, electricity, hydrogen and dry air. In this plan, the net exergy and energy efficiency of this system increased while the operation and maintenance cost of the cycle decremented. In multi-generation cycles, the electricity can transfer to the customers with minimum cost but the efficiency slump nearly 9% due to dispensation (Khaliq, Kumar, & Dincer, 2009). For designating a proper and feasible multi-generation plant, the economic assessments like initial and operation costs should be considered to bind the usefulness of the system. An integrated collation procedure for finding the thermal efficiency of multi-generation utilities has carried out by Athanasovici et al. (Athanasovici, Le Corre, Brecq, & Tazerout, 2000). Havelsky (Havelský, 1999) studied the obstacle of energy performance appraisal of plants for various outputs.

Ahmadi et al. (Ahmadi, Dincer, & Rosen, 2011) performed energy, exergy, and different intention optimization of multi-generation plants to achieve best design factors. An exergy investigation of the combination of electrical power and refrigeration plant studied by Khaliq et al. (Khaliq et al., 2009). Energy and exergy assessment of renewable energy-based multi-generation with various outputs carried out by Dincer and Zamfirescu (Murphy & Niitsuma, 1999).

2.2 Geothermal Energy

Geothermal energy is an environmentally friendly and sustainable power source, as mentioned by Murphy et al. (Fridleifsson, 2001). From 1913, generating electricity commercially by geothermal energy has been started and since 1950 many of MW for electricity produced. In 2000, the capability of 80 countries for using the geothermal energy had recognized among which 58 of them exploited this renewable energy. 54 TWh/a, for domestic application and 49TWh/a, of electricity have been count as the usage of geothermal energy in the world. Just 21 countries can produce electricity by geothermal steam in which only 5 of them acquire 10-22% of their need from this source of energy (Dickson & Fanelli, 2013). Gaining temperature with profundity in the Earth's cortex called as geothermal tilt. The mean of the geothermal gradient is nearly 2.5 to 3 °C/100m by using modern technologies and drill (Fridleifsson, 2003). There are various scenarios for consensus the energy demand in the future by the World Energy Council (WEC) which focused on the development of technology, environmental conservation, international justice and economic growth rate. These scenarios appoint because of better energy efficiency and suitability of environment. From 1990 to 2050, the central expenditure of energy is expected to rise nearly 50% based on the conscious scenario and 275% relevant to highest growth rate scenario (Lund, Freeston, & Boyd, 2011). As long as the use of

6

geothermal energy is detected, its usage has risen nearly double as pointed by various researchers (Jalilinasrabady & Itoi, 2013; Kanoglu & Bolatturk, 2008; Ozgener, Hepbasli, & Dincer, 2005). Typically there are three different class for origins of geothermal energy based upon origin temperatures where minimum temperature origin is less than 89 °C, medium temperature origin is between 89 and 149 °C and maximum temperature source is more than 149 °C (Ozgener et al., 2005). Geothermal energy usages such as electricity production, heating, cooling and drying have analyzed by Ozgener et al. (Tchanche, Lambrinos, Frangoudakis, & Papadakis, 2010).

There are significant advantages for geothermal energy as below:

a) Economic aspect:

Geothermal energy usually contains low running cost because no fuel is needed and the side costs such as transportation of fuels or refining the plant are completely skimp. Also as the governments are investing in this system, it can increase the job opportunities in proper places.

b) Reduction in reliability on fossil fuels:

Since geothermal energy is a RES with minimum pollution, environmental side effects and because of the minor operating cost, it is logical to develop it and decrease reliability on fossil fuels.

c) Minimum emission:

The geothermal energy does not produce any emission and this is the primary benefit of using such utilities, so this renewable source of energy can help the world to reduce global warming.

d) Practical for cooling and heating:

The diversity among temperature of the surface and the ground source is significant. As a result, the field can operate as a heat sink coupled to a heat pump to produce heating and cooling relatively.

There are some disadvantages for geothermal energy which are listed as follow:

a) Not common energy source:

Because this type of energy not developed yet there are some issues in the availability of the proper equipment's and professional staffs which leads to massive problems in installation and developing such systems in the world.

b) High investment needed:

For running the geothermal energy the power plant is necessary and to attain steam from profound through the earth massive investment required to drill and locate the particular position for the plant which increases the cost of this renewable source of energy. As it is clear, the effects of the geothermal energy are considerable and consequently increase the tendency to invest in this system.

2.3 ORC

The ORC is one of the most identified technologies in the power engineering field which is proper for altering the energy. In this system vapor, steam replaced by some flowing such as refrigerants and hydrocarbons. Operating in the small scale applications and heat recovery in low temperature are some of the privileges of the ORC (Angelino, Gaia, & Macchi, 1984). The advancement of the ORC has started from early 19th century and has continued until today which is popular in the sustainable energy market. The development of the steam reciprocating engines raised up rapidly in the early 19th century. The growth of the ORC was under

presence of steam reciprocating engines. Because of the pressure limits in the boilers on those days, alternative fluids used which bounded the highest temperature of the cycle so for solving that problem no aqueous fluids exerted. Given the fact that sealing methods were insufficient because of the high temperature of the heat sink, achieving admissible condenser vacuum was a formidable task. First attempt to utilize the organic fluid in an actual turbine was made by Prof. Luigi D'Amelio (1935), and it was the beginning of the revolution of the ORC (Borsukiewicz-Gozdur & Nowak, 2007).

ORC typically contains pump, regenerator, evaporator, turbine, generator and condenser which the working principles of each of them will illustrate in following steps. The aim of using a pump is to transfer the organic fluid into a regenerator which can less superheat the vapor as a preheating process. After that, the preheated fluid evaporated, superheated and finally expanded in the turbine which can run the generator of the system. In the condenser, the less superheated vapor condensed. For the utmost temperature level, the heat recovery can be beneficial for the finite heating net but if the temperature for running the ORC be low, the cooling water can cool the condenser. Depends on the application and heat lost amount, the proper working flowing for the ORC can be designated which is the considerable part of this system (Secretariat, 2006). The ORC can run by saturated vapor or by some superheated fluids. Since the distension of many fluids finishes in the superheated vapor position, high superheating is not intransitive. For achieving higher efficiency higher superheating is required but since little heat exchange coefficient can accomplish only by large and costly heat exchangers, it is not economical to use. Another primary factor that cannot ignore alongside the thermodynamic properties is administrative actions about the detriment of working fluid. These statutes used to

detract emission of greenhouse gasses and preserve ozone layer (Devotta & Holland, 1985). The ORC is not a novel notion, and many analyses have done (DiPippo, 2012). Typical usages apply geothermal (Maizza & Maizza, 2001) or heat lost (Liu, Chien, & Wang, 2004). It has also examined as a plant integrated with gas turbines or various intense temperature plants. A thermodynamic assessment for a biomass cogeneration cycle according to ORC has performed by Al-Sulaiman et al. (Izquierdo, Lizarte, Marcos, & Gutiérrez, 2008).

2.4 SEAC

Condensation and evaporation of a refrigerant are the basis of absorption and vapor compression technologies toward heating and cooling. The electricity is the energy source for modern work to compress the vapor, while in the chiller, heat of the utility is transferred to the generator directly (Ali, Noeres, & Pollerberg, 2008). Ordinary air-conditioning systems need superior energy and electricity produced by leading energy sources. Although, notwithstanding of cooling liquid of Chlorofluorocarbon (CFC), the saving of energy and emission rate are ascending. As a matter of fact, accessing of renewable energy propose an occasion to operate green energy for cooling (Kim & Park, 2007). SEAC pursuant to the Lithium-bromide water devised in the 1950s (Ward, Löf, & Uesaki, 1978). Single effect absorption chiller according to lithium bromide-water is the most common system in this area because of its ability to work on small temperature ranges (Aphornratana & Sriveerakul, 2007) . The fluid which used in the refrigeration system contains absorbent and refrigerant. Let assume two containers which one of them comprise of lithium bromide water solution and the other one consist of liquid water as a refrigerant. The solution can imbibe water vapor and because of vaporization reduce the temperature of the debris solution. In this time, refrigeration falls out in the refrigerant container and solution

becomes diluted since the amount of water absorbed is extremely more than the previous condition. This process named as absorption (Florides, Kalogirou, Tassou, & Wrobel, 2002). In the absorption process, the desiccant experiences a chemic altering because of receiving the dampness, which makes it extremely beneficial in the separation procedure (Bessah & Benyoussef, 2015). As a privilege, the SEAC can run in low temperature from 80 to 110 °C with flat collectors which results in efficacious and minor cost.

2.5 Electrolysis

Electrolysis is plainly exerting electricity to disintegrate water to hydrogen gas and oxygen gas (Andújar & Segura, 2009). Electrolyser deciphered nearly two hundred years ago via Nicholson and his colleague (Zeng & Zhang, 2010) whilst leading hydrogen gas generation till now (Ott, 1994). In electrolysis water detaches into positive and negative ions (Harris, 2010) while the positive ions are imbibed to the negative electrode and diminished to a single hydrogen. The procedure is extremely labile and instantly reacts with the further hydrogen atom to conduct molecular hydrogen gas (H_2) (Hovsapian et al., 2008). At another electrode, oxidation happens. The negative ions imbrued to the positive electrode in position that oxygen gas and hydrogen ions generated. One of the primary purposes of using electrolysis is to use it in a proton exchange membrane (PEM) to produce electricity even at night. According to the investigation by particular researchers (Ghosh, Emonts, Janßen, Mergel, & Stolten, 2003; Hollmuller, Joubert, Lachal, & Yvon, 2000; Yilanci, Dincer, & Ozturk, 2008, 2009) various renewable sources of energy like, solar energy is a source of hydrogen generation. Hydrogen will be a significant parameter shortly as a part of sustainable energy progress since it is environmentally friendly and provide water at the end (Asghari, Mokmeli, & Samavati, 2010; Barelli, Bidini,

Gallorini, & Ottaviano, 2011; I Dincer & Zamfirescu, 2012; Ibrahim Dincer, 2007;

Ni, Leung, & Leung, 2007).

Chapter 3

SYSTEM DESCRIPTION AND METHODOLOGY

3.1 System description

The boiler is a source of the geothermal energy in which the whole of the system can

run by fluid that goes through it. In this cycle liquid n-pentane passes among a boiler

at (17) and it phase changes to superheated fluid at (3). After that this fluid will go to

the turbine to conjugate most of its energy (enthalpy) for rotating the turbine blades.

By rotating the blades it can produce energy needed for running the generator and at

that point generator can produce 24.98 kW electricity needed for the cycle.

Depending on the demand 12.5 kW of electricity can be used in home applications

and the rest for running the electrolyzer. The aim of producing hydrogen is to store

generated excess electricity for later use also chemical industries use it for

hydrochloric acid production as well as for atomic hydrogen welding (AHW). It is

also used in the food and chemical industries. Food industries use the element to

make hydrogenated vegetable oils such as margarine and butter. In this procedure,

vegetable oils are combined with hydrogen. When a direct current voltage is applied

to the electrolyzer, water molecules at the anode are oxidized to oxygen and protons,

while electrons are released. The protons (H^+ ions) pass through the PEM to the

cathode where they meet electrons from the other side of the circuit, reducing to

hydrogen gas (Stojić, Marčeta, Sovilj, & Miljanić, 2003). At point 4 the enthalpy of the fluid decreased but it is still superheated fluid. This fluid goes to the generator-II to give its energy and become cooler and at the end pumps to the boiler for completing the cycle. At points 5 to 6 the stepper is used to make sure that the phase of the fluid is absolutely saturated liquid and there is no gaseous phase on it. The generator-II is a heat source in the SEAC system and the fluid which is used is Libr-Water. At point (9) this fluid goes to the generator-II and after absorbing heat from generator some of the water of fluid transferred to the superheated gas and goes out from point (13), as well as, more concentrated fluid goes off from point 10 to enter the heat exchanger to giving the heat. This fluid goes off to the expansion valve to reduce the pressure at spot (11) and then enter the absorber at (12). At point (13) water vapor is condensed in the condenser and after passing over from expansion valve (14) because of reduction in pressure some of water molecules vaporized and create a mixture at (15). By passing the water mixture from evaporator and gaining heat it gives cold to the environment which this cold fluid is used in air conditioning system and also for drying the air. The hot and wet air enters the AC and after passing across it transfers heat to it because the purpose is to decrease dew point of the system, in which pressure and temperature detract at the same time and change the air to liquid. The concentrated solution from point (12) and pure water of (16) mixed together in absorber and form the diluted solution at spot (7).

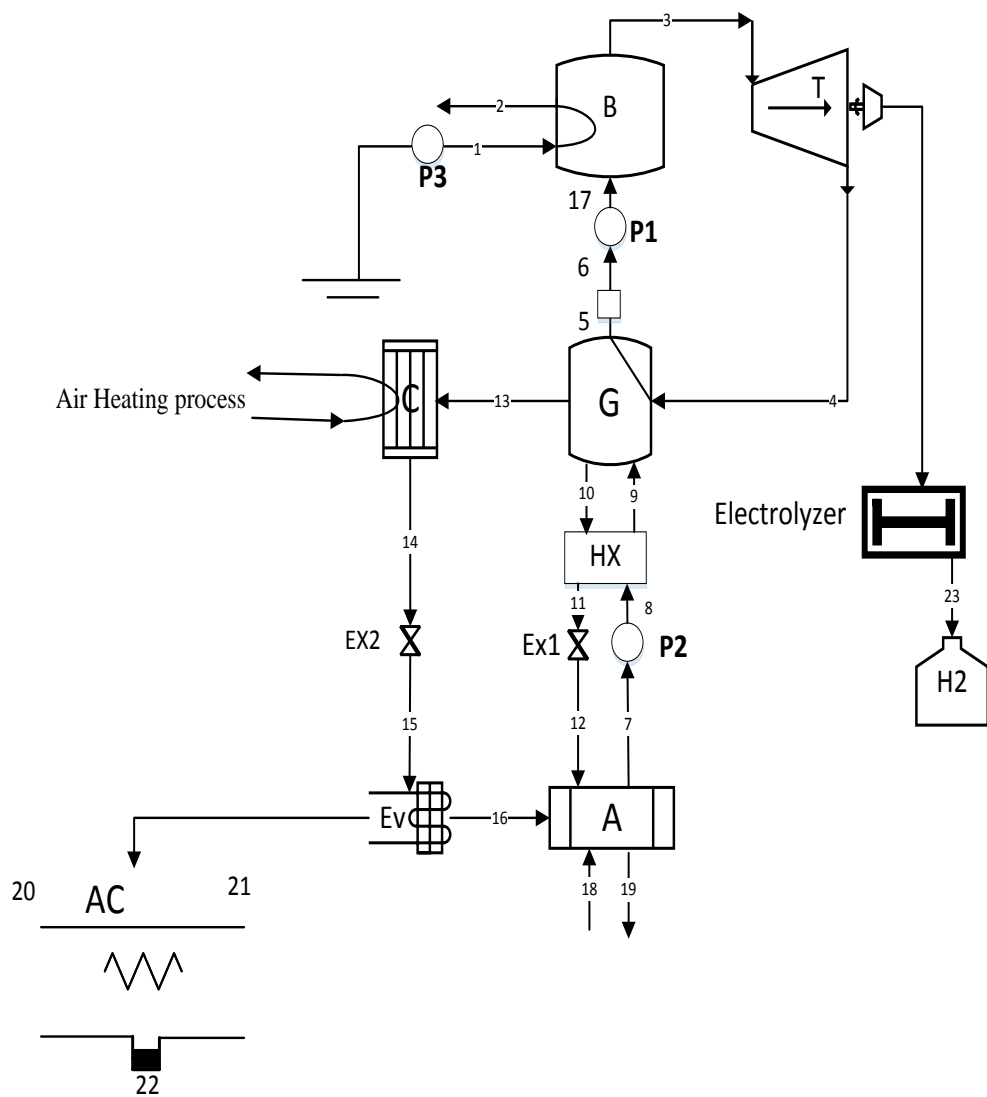As illustrated, the schematic of the system shown in the Figure 3.1.

Figure 3.1 Schematic of the system

Table 3.1: Description of system components in the schematic

Abbreviation	Description
B	Boiler
T	Turbine
P	Pump
H	Electrolysis
G	Generator
C	Condenser
HX	Heat Exchanger
EX	Expansion Valve
A	Absorber
EV	Evaporator
AC	Air conditioning

Table 3.2: Description of flow numbers

Flow number	Description of flow
1	Geothermal water flow enters to the boiler
2	Geothermal water flow leaves the boiler
3	Superheated steam leaves the boiler
4	Outlet steam flow leaves the turbine
5	Condensed saturated liquid water goes out from generator
6	Condensed saturated liquid water goes out from generator
7	Strong libr-water solution leaves the absorber
8	Strong libr-water solution pumped through the heat exchanger
9	Strong libr-water solution enters to the generator
10	Weak libr-solution goes into the heat exchanger
11	Weak libr-solution goes out of the heat exchanger
12	Expanded weak libr-solution enters to the absorber
13	Separated superheated steam leaves the generator
14	Condensed water goes out of the condenser
15	Expanded mixed saturated water enters to the evaporator
16	Superheated low pressure water vapor leaves the evaporator
17	High pressure saturated water goes into the boiler

18	Supplied water goes to the absorber
19	Hot water goes out of the absorber
20	Hot and wet air enters the air conditioner
21	Cold and dry air produced by air conditioner
22	Moisture
23	Hydrogen produced by the electrolysis

3.2 Methodology

Energy and exergy balance of various elements in the utility has developed moreover overall energetic and exergetic efficiencies of the system were analyzed through the development of thermodynamic models. For performing this study the engineering equation solver (EES) has been used to analyze the thermal properties of the system since the software is well known for this purpose. For this assessment there are some assumption which are listed as below:

1. All points and components in the cycle are steady.

2. Heat lose and pressure drops of all the pipes and equipment considered negligible.

3. The environment state is defined by a pressure of $P_0 = 100$ kPa and a temperature of $T_0 = 293.15$ K.

4. Because the gases in the system are in low pressure and high temperature, produced gases and air are considered as an ideal-gas mixtures.

5. In order to investigate the maximum potential of performance system components assumed as isentropic thereby any irreversibility is neglected.

In the following table the variables of various parameters in the study illustrated.

Table 3.3: Description of assumptions

Parameter	variable
Turbine inlet pressure	2000 kPa
Mass flow rate of ORC fluid	0.498 kg/s
Strong solution concentration	56.94
Weak solution concentration	52.25
Inlet temperature of water heating	104.8 K
Mass flow rate of water heating	8.471 kg/s
Upper pressure of absorption unit	4.81 kPa
Down pressure of absorption unit	1 kPa
Temperature of superheated steam in generator	340.2 K
Electrolyzer efficiency	0.54
Relative humidity in AC inlet	0.84
Geothermal source mass flow rate	11.88 kg/s
Geothermal source temperature	483.2 K
Electricity ratio supplied to electrolyzer	0.5
Exhaust geothermal temperature	463.2 K

In the next section energy and exergy assessment for this study are demonstrated.

3.2.1 Pump 1 analysis
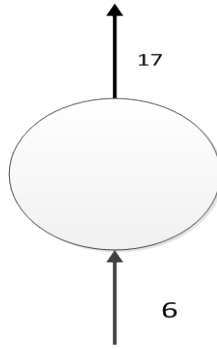
The schematic of the pump 1 shows in Figure 3.2.
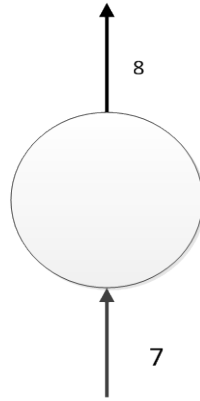

Figure 3.2: Schematic of pump 1

The below equations represent information about the pump 1:

$$\dot{m}_{17} = \dot{m}_6 \tag{1}$$

$$\dot{W}_{pump,1} = \dot{m}(h_{17} - h_6) \tag{2}$$

$$\dot{W}_{pump,1} = \dot{m}_6 \times v_6(p_{17} - p_6) \tag{3}$$

$$Ex_6 + \dot{W}_{pump,1} = Ex_{17} + \dot{Ex}_{d,pump,1} \tag{4}$$

Where $\dot{W}_{pump,1}$, $\dot{m}_i$, v_i, p_i, h_i, $\dot{Ex}_{d,pump,1}$ and Ex_i represent pump work, mass flow rate, specific volume, pressure, enthalpy, exergy destruction rate and state exergy, respectively.

3.2.2 Pump 2 analysis

The schematic of the pump 2 shows in the Figure 3.3;

Figure 3.3: Schematic of pump 2

The below equations represent information about the pump 2:

$$\dot{m}_8 = \dot{m}_7 \tag{5}$$

$$\dot{W}_{pump,2} = \dot{m}(h_8 - h_7) \tag{6}$$

$$\dot{W}_{pump,2} = \dot{m}_7 \times v_7(p_8 - p_7) \tag{7}$$

$$Ex_7 + \dot{W}_{pump,2} = Ex_8 + \dot{Ex}_{d,pump,2} \tag{8}$$

Where $\dot{W}_{pump,2}$, $\dot{m}_i$, v_i, p_i, h_i, Ex_i, and $\dot{Ex}_{d,pump,2}$ represent pump work, mass flow rate, specific volume, pressure, enthalpy, state exergy and exergy destruction rate, respectively.

3.2.3 Boiler analysis

Geothermal water flow goes into the boiler at point (1) and leaves boiler at (2) while, high pressure saturated water goes into the boiler (17) and leaves the boiler as a superheated steam. The Figure 3.4 shows the boiler schematics;
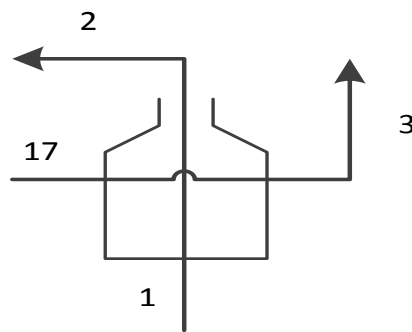

Figure 3.4: Schematic of boiler.

The following formulas illustrate boiler analysis:

$$\dot{Q}_{boiler} = \dot{m}_{17}h_{17} - \dot{m}_3h_3$$

(9)

$$\dot{Q}_{boiler} = \dot{m}_2h_2 - \dot{m}_1h_1$$

(10)

$$\dot{Ex}_{boiler} = (1 - \frac{T_0}{T_{avg}})\dot{Q}_{boiler}$$

(11)

$$T_{avg} = \frac{(T_1+T_2+T_3+T_{17})}{4}$$

(12)

$$Ex_1 + Ex_{17} = Ex_2 + Ex_3 + \dot{Ex}_{d,boiler} \tag{13}$$

Where, $\dot{Q}_{boiler}$, $\dot{m}_i$, h_i, $\dot{Ex}_{boiler}$, T_0, T_{avg}, $\dot{Ex}_{d,boiler}$ and Ex_i shows, heat flow rate of boiler, mass flow rate, enthalpy, thermal exergy rate, ambient temperature, average temperature, exergy destruction rate and exergy, respectively.

3.2.4 Turbine analysis

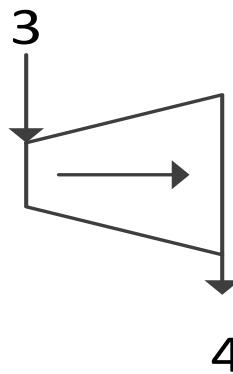The turbine schematic shows in the Figure 3.5:

Figure 3.5: Schematic of turbine.

The given equations show turbine analysis:

$$W_{turb} = \dot{m}_3(h_4 - h_3)$$

(14)

$$\dot{Ex}_{d,turb\ 1} = Ex_3 - W_{turb} - Ex_4 \tag{15}$$

In which, W_{turb}, $\dot{m}_i$, h_i, $\dot{Ex}_{d,turb\ 1}$ and Ex_i present, total work of turbine, mass flow rate, enthalpy, exergy destruction rate and exergy, subsequently.

3.2.5 Generator analysis

The schematic of generator is presented in the Figure 3.6.
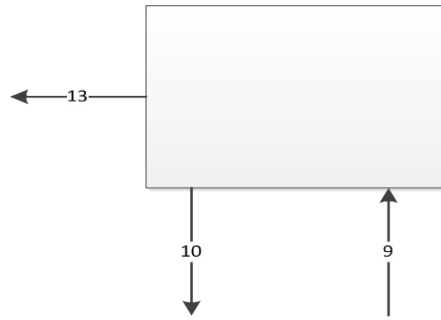

Figure 3.6: Schematic of generator.

The equations related to the generator are as below:

$$\dot{Q}_{gen} = \dot{m}_{10}h_{10} + \dot{m}_{13}h_{13} - \dot{m}_9h_9 \tag{16}$$

$$\dot{Q}_{gen} = \dot{m}_4(h_4 - h_5) \tag{17}$$

$$Ex_{gen} = (1 - \frac{T_0}{T_{avg}})\dot{Q}_{gen} \tag{18}$$

$$T_{avg} = \frac{(T_{10} + T_{13} + T_9)}{3} \tag{19}$$

$$\dot{Ex}_{d,gen} = Ex_9 - Ex_{10} - Ex_{13} + Ex_{gen} \tag{20}$$

Where, $\dot{Q}_{gen}$, $\dot{m}_i$, h_i, Ex_{gen}, T_0, T_{avg}, $\dot{Ex}_{d,gen}$ and Ex_i shows, heat flow rate of generator, mass flow rate, enthalpy, thermal exergy rate, ambient temperature, average temperature, exergy destruction rate and exergy, respectively.

3.2.6 Heat exchanger analysis

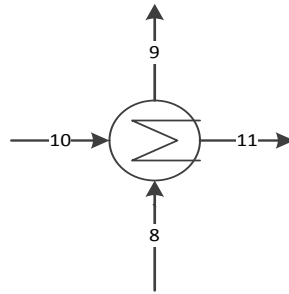The schematic of heat exchanger illustrated in Figure 3.7;

Figure 3.7: Schematic of heat exchanger.

The equations below indicate heat exchanger analysis:

$$\dot{m}_8 h_8 + \dot{m}_{10} h_{10} = \dot{m}_9 h_9 + \dot{m}_{11} h_{11} \tag{21}$$

$$\dot{Q}_{HX} = \dot{m}_{10} h_{10} - \dot{m}_{11} h_{11}$$

(22)

$$\dot{Ex}_{HX} = (1 - \frac{T_0}{T_{avg}})\dot{Q}_{HX}$$

(23)

$$T_{avg} = \frac{(T_8 + T_9 + T_{10} + T_{11})}{4}$$

(24)

$$\dot{Ex}_{d,HX} = Ex_{10} + Ex_8 - Ex_{11} - Ex_9 + \dot{Ex}_{HX} \tag{25}$$

In which, $\dot{Q}_{HX}$, $\dot{m}_i$, h_i, $\dot{Ex}_{HX}$, T_0, T_{avg}, $\dot{Ex}_{d,HX}$ and Ex_i shows, heat flow rate of heat exchanger, mass flow rate, enthalpy, thermal exergy rate, ambient temperature, average temperature, exergy destruction rate and exergy, respectively.

3.2.7 Absorber analysis

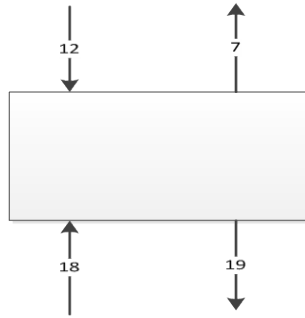The schematic of the absorber represented by the Figure 3.8.

Figure 3.8: Schematic of absorber

The following equations present absorber analysis:

$$\dot{Q}_{abs} = \dot{m}_{12}h_{12} + \dot{m}_{16}h_{16} - \dot{m}_7h_7 \tag{26}$$

$$\dot{Q}_{abs} = \dot{m}_{18}(h_{18} - h_{19})$$

(27)

$$Ex_{abs} = (1 - \frac{T_0}{T_{avg}})\dot{Q}_{abs} \tag{28}$$

$$T_{avg} = \frac{T_{12}+T_{16}+T_7}{3}$$

(29)

$$\dot{Ex}_{d,abs} = Ex_{16} + Ex_{12} - Ex_7 - Ex_{abs} \tag{30}$$

Where, $\dot{Q}_{abs}$, $\dot{m}_i$, h_i, Ex_{abs}, T_0, T_{avg}, $\dot{Ex}_{d,abs}$ and Ex_i represent, heat flow rate of absorber, mass flow rate, enthalpy, thermal exergy rate, ambient temperature, average temperature, exergy destruction rate and exergy.

3.2.8 Condenser analysis

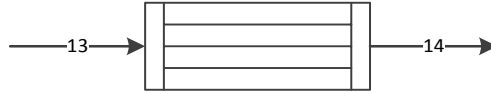The schematic of condenser is given in Figure 3.9 as follow:

Figure 3.9: Schematic of condenser.

The equations of condenser are given by:

$$\dot{Q}_{cond} = \dot{m}_{13}h_{13} - \dot{m}_{14}h_{14} \tag{31}$$

$$Ex_{cond} = (1 - \frac{T_0}{T_{avg}})\dot{Q}_{cond} \tag{32}$$

$$T_{avg} = \frac{T_{13}+T_{14}}{2}$$

(33)

$$\dot{Ex}_{d,cond} = Ex_{13} - Ex_{14} + Ex_{cond} \tag{34}$$

In which, $\dot{Q}_{cond}$, $\dot{m}_i$, h_i, Ex_{cond}, T_0, T_{avg}, $\dot{Ex}_{d,cond}$ and Ex_i present, heat flow rate of condenser, mass flow rate, enthalpy, thermal exergy rate, ambient temperature, average temperature, exergy destruction rate and exergy.

3.2.9 Evaporator analysis
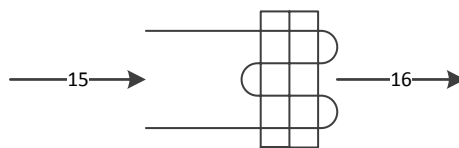
In the Figure 3.10 the schematic of evaporator is given;

Figure 3.10: Schematic of evaporator.

The equations about the evaporator are presented as follow:

$$\dot{Q}_{Evap} = \dot{m}_{15}h_{15} - \dot{m}_{16}h_{16}$$

(35)

$$Ex_{Evap} = (1 - \frac{T_0}{T_{avg}})\dot{Q}_{evap}$$

(36)

$$T_{avg} = \frac{T_{15} + T_{16}}{2}$$

(37)

$$\dot{Ex}_{d,Evap} = Ex_{16} - Ex_{15} + Ex_{Evap} \qquad (38)$$

In which case, $\dot{Q}_{Evap}$, $\dot{m}_i$, h_i, Ex_{Evap}, T_0, T_{avg}, $\dot{Ex}_{d,Evap}$ and Ex_i demonstrate mass flow rate of evaporator, mass flow rate, enthalpy, thermal exergy rate, ambient temperature, average temperature, exergy destruction rate and exergy, respectively.

3.2.10 Electrolyzer analysis
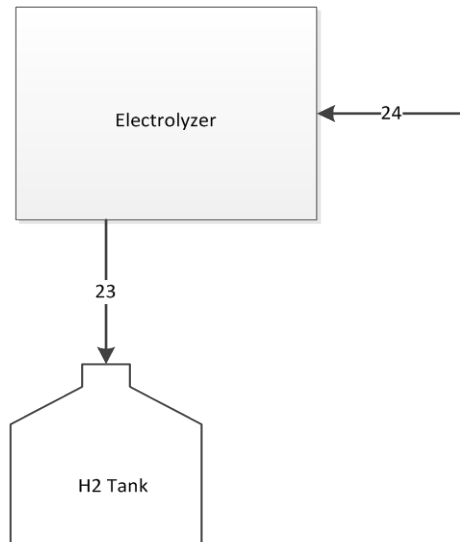
The Figure 3.11 shows the schematic of electrolyzer;

Figure 3.11: Schematic of electrolyzer.

The below equations illustrate analysis of electrolyzer:

$$\dot{m}_{24} = \dot{m}_{23} \tag{39}$$

$$\dot{m}_{H_2} = \frac{\eta_{elect} \times W_{net}}{HHV}$$

(40)

$$Ex_{ph,H_2} = (h_{23} - h_0) - T_0(s_{23} - s_0) \tag{41}$$

$$Ex_{ch,H_2} = (236.09 \times 1000)/MW \tag{42}$$

In which, the related table for Ex_{ch,H_2} is given in appendix B which shows that 236.09 kJ/kmol is the chemical exergy of the hydrogen.

$$Ex_{H_2} = \dot{m}_{H2}(Ex_{ph,H_2} + Ex_{ch,H_2})$$

(43)

$$Ex_{d,H_2} = Ex_{24} - Ex_{H_2}$$

(44)

In which, $\dot{m}_{H_2}$, η_{elect}, W_{net}, HHV, Ex_{ph,H_2}, h_i, T_0, s_i, Ex_{ch,H_2}, MW, Ex_{H_2}, Ex_{d,H_2} are mass flow of hydrogen produced, mass flow of water, efficiency of electrolyzer, total work, high heating value, physical exergy, enthalpy, ambient temperature, entropy, chemical exergy, molar mass, exergy and exergy destruction rate, accordingly.

3.2.11 Dehumidification analysis
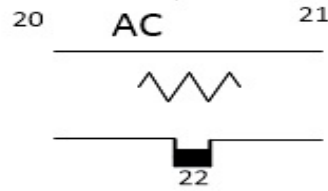
The Figure 3.12 shows dehumidification system;

Figure 3.12: Schematic of dehumidification system.

The analysis of dehumidification system is as follow:

$$\eta_{dehumid} = \left(\frac{\dot{m}_{air,21} h_{21}}{\dot{Q}_{dehumid}}\right) \times 100 \tag{45}$$

$$\dot{m}_{air,20} \times W_{20} = \dot{m}_{air,21} \times W_{21} + \dot{m}_{water} \tag{46}$$

$$\dot{Q}_{dehumid} = \dot{m}_{air,21} \times (h_{20} - h_{21}) - \dot{m}_{water} h_{water} \tag{47}$$

$$T_{avg} = \frac{T_{20} + T_{21}}{2}$$

$$\tag{48}$$

$$Ex_{dehumid} = \left(1 - \frac{T_0}{T_{avg}}\right) \times \dot{Q}_{dehumid} \tag{49}$$

$$\dot{Ex}_{d,dehumid} = Ex_{20} - Ex_{21} - Ex_{22} - Ex_{dehumid} \tag{50}$$

Where, $\eta_{dehumid}$, $\dot{m}_{air,i}$, h_i, T_0, $\dot{Q}_{dehumid}$, W_i, $\dot{Ex}_{d,dehumid}$, T_{avg}, $Ex_{dehumid}$ and Ex_i, represent efficiency of dehumidification system, mass flow rate of air, enthalpy,

ambient temperature, heat flow rate of dehumidification, specific humidity, thermal exergy, average temperature, exergy destruction rate and exergy.

3.2.12 Analysis of system

The following equations represent coefficient of performance in energy and exergy term of whole system, energetic and exergetic of the system and also the efficiency of organic Rankine cycle respectively.

$$COP_{en} = \frac{\dot{Q}_{Evap} + \Sigma \dot{Q}_{cond}}{\dot{Q}_{geo} + \Sigma W_{pump}} \qquad (51)$$

$$COP_{ex} = \frac{Ex_{Evap} + \Sigma Ex_{cond}}{\dot{Ex}_{geo} + \Sigma W_{pump}} \qquad (52)$$

$$\eta_{ORC} = (\frac{W_{net}}{\dot{Q}_{in}}) \times 100 \qquad (53)$$

$$\eta_{en} = \frac{\dot{m}_{23} HHV + \dot{Q}_{Evap} + Elect + \dot{Q}_{Abs} + \dot{Q}_{Cond}}{Q_h} \qquad (54)$$

$$\eta_{ex} = \frac{Ex_{Cond} + Ex_{H2} + Ex_{Evap} + Ex_{Abs} + Elect}{Ex_{input}} \qquad (55)$$

`

Chapter 4

RESULTS AND DISCUSSION

As illustrated in pervious chapters, because of the disadvantages of fossil fuels such as, greenhouse gasses, high emission and price the tendency to developing renewable energy increased. One of these alternatives is using multi-generation system which runs with geothermal source but the major obstacle is that geothermal is only available in certain locations. As a result, other origins of energy such as biomass and solar can be used instead.

In the present project, a system with geothermal source was designed to generate heat for running the Organic Rankine cycle and produce heat, cooling and also electricity for home applications and to turn out hydrogen by electrolyzer. Moreover, it can produce dry air by air conditioning system of SEACS. In this research, energetic and exergetic analysis of various parameters in addition to ambient temperature, turbine inlet pressure, hydrogen production rate and coefficient of performance have been studied. According to first law of thermodynamic energy can transfer from one form to another but quality of it will alter. Although, by experience, outlet energy is always less than inlet because of loss of energy (Bereche, Palomino, & Nebra, 2009; Gebreslassie, Medrano, & Boer, 2010; Niksiar & Rahimi, 2009). The primarily purpose of analyzing the energy is to specify the exploited and

lost energies. Since a few years ago, new definition which is called exergy and is related to capability of various energy to work has been developed. Because of thermodynamic irreversibility, the exergy efficiency of a system is smaller than an energy efficiency which shows the quality decay of various energies (Şencan, Yakut, & Kalogirou, 2005). Using multi-generation system enables to utilize the low grade energy, reduce waste heat thereby improves the exergetic efficiency of the system.

The primarily parameters which have been studied are illustrated in Table 4.1. To accredit the study, results are compared with a system which presented by (Ahmadi et al., 2011) and compared in the Table 4.1.

Table 4.1: Comparing the result of present thesis with work done by other researchers.

Studied Parameters	Present Study	Previous Study
η_{en}	1.59	1.68
η_{ex}	0.4121	0.33
$\eta_{Electrolyzer}$	0.56	-
COP_{en}	0.8419	1.63 (DEAC)
COP_{ex}	0.4692	0.3
Dehimidifing energy	6126 kW	-
$\dot{Q}_{heating}$	248 kW	1487 kW
$\dot{Q}_{cooling}$	224.3 kW	2000 kW
$\dot{m}_{hotwater}$	8.471 kg/s	0.52 kg/s
$\dot{m}_{H_2}$	0.3538 kg/s	1.19 kg/s
Electricity produced	24.98 kW	287 kW
Total exergy destruction	305.7 kW	3749 kW

Based on the results of the above table it is clear that the energetic and exergetic efficiencies of both studies are nearly same while COP_{en} is twofold of this assessment because in other study the double effect absorption chiller have been used.
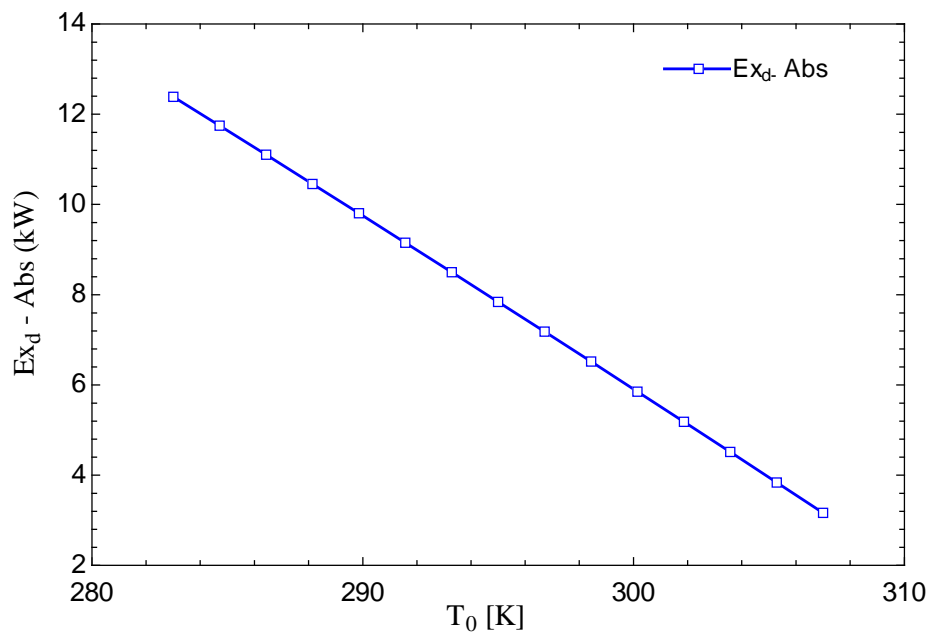
4.1 Analyzing the effect of ambient temperature on exergy destruction

4.1.1 Effect of ambient temperature on exergy destruction in the absorber

As shown in the Figure 4.1, by increasing the ambient temperature from 283 K to 308K, the exergy destruction of the absorber will decrease from 12.4 kW to nearly 3 kW. So the high performance of the absorber occur at lower temperatures moreover, it is beneficial to deliver water with higher mass flow rate and lower temperature to achieve premier efficiency.

Figure 4.1: Effect of ambient temperature on exergy destruction in absorber

4.1.2 Effect of ambient temperature on exergy destruction in the condenser

In the Figure 4.2 the correlation among ambient temperature and exergy destruction of the condenser presented. As it is clear the exergy destruction of the condenser dropped from 46 kW to nearly 10 kW. The ambient temperature range is between 283 K and 308 K. Since the minimum exergy destruction of the condenser is from 300 K to 308 K it is better to run in in this interval.
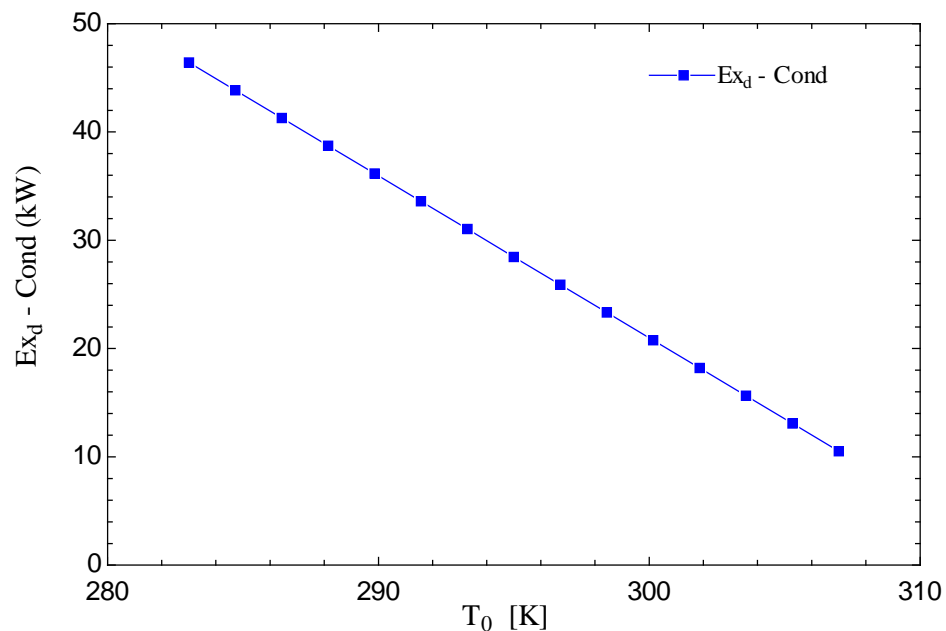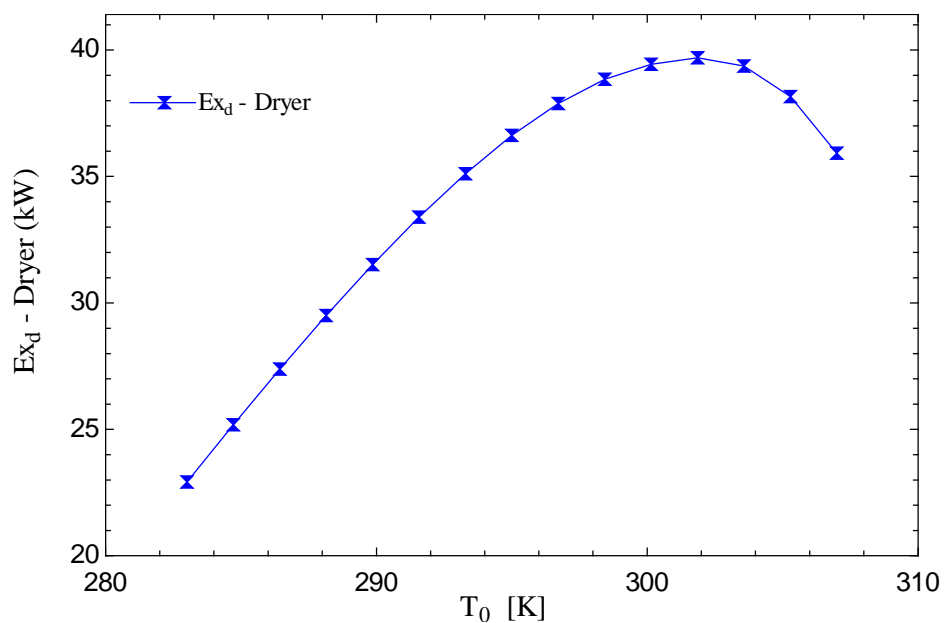

Figure 4.2: Effect of ambient temperature on exergy destruction in condenser

4.1.3 Effect of ambient temperature on exergy destruction in the dryer

In the Figure 4.3 the effect of the ambient temperature on the exergy destruction of the dryer is presented. In this graph exergy destruction will rise by increasing the ambient temperature until 302 K which is the critical point for exergy destruction and after that point there is a noise diving and it will continue to decline. The ambient temperature range is from 283 to 308 and the period of the exergy destruction is between 23 kW and 40 kW. Therefore the most efficient interval for dryer is among 283 K to 290 K. Since the increasing of input exergy is more than rising of useful exergy of cooling the drop after the critical point is logic.
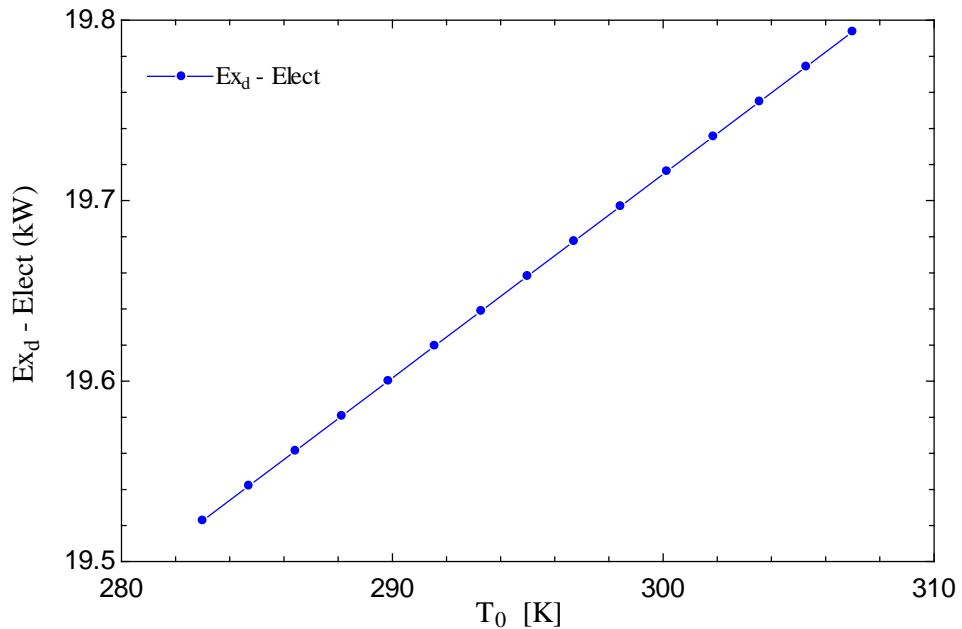

Figure 4.3: Effect of ambient temperature on exergy destruction in dryer

4.1.4 Effect of ambient temperature on exergy destruction in the electrolyzer

In the Figure 4.4 the impact of the ambient temperature on the exergy destruction of electrolyzer is shown. The graph experience a steady growth from 19.5 kW to 19.8 kW for exergy destruction of the electrolyzer and amongst 283 K to 308 K for the ambient temperature. Since the best performance of electrolyzer is at minimum exergy destruction, it should run between 283 K and 290 K. By reducing the ambient temperature it is possible to reduce the exergy destruction but too much reduction would lead to face negative effect of temperature reduction in other words, it requires more electricity to decompose the water molecules.
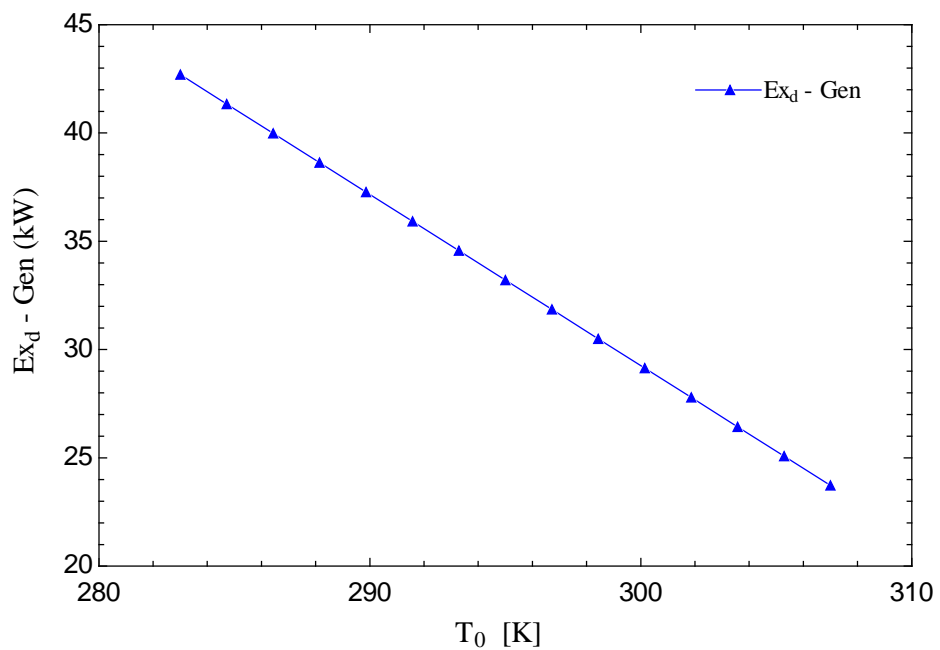

Figure 4.4: Effect of ambient temperature on exergy destruction in electrolyzer

4.1.5 Effect of ambient temperature on exergy destruction in the generator

In the Figure 4.5 the effect of the ambient temperature on the destruction exergy of the condenser presented. According to the figure the exergy destruction of the condenser dropped from 43 kW to 23 kW. The ambient temperature range is between 283 K and 308 K. Since the minimum exergy destruction of the generator is from 300 K to 308 K it is better to run in in this interval. Since the generator works in a position with high ambient temperature so downward trend in exergy destruction is beneficial.
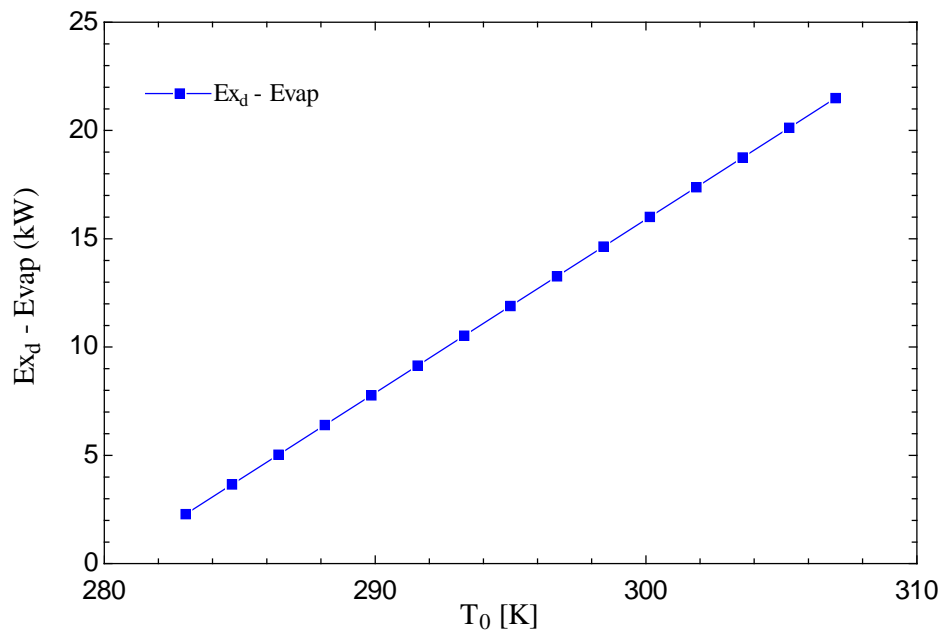

Figure 4.5: Effect of ambient temperature on exergy destruction in generator

4.1.6 Effect of ambient temperature on exergy destruction in the evaporator

The impact of the ambient temperature on the exergy destruction of evaporator is shown in the Figure 4.6. The graph picks up continuously from 2 kW to 20 kW for exergy destruction of the evaporator and between 283 K and 308 K for the ambient temperature. The best performance of evaporator is between 283 K and 290 K. Since the aim of using evaporator is cooling, so it affect negatively by implementing the evaporator in high ambient temperature.

Figure 4.6: Effect of ambient temperature on exergy destruction in evaporator

4.1.7 Effect of ambient temperature on exergy destruction in the turbine

Based upon in the Figure 4.7, by increasing the ambient temperature from 283 K to 308K, the exergy destruction of the turbine will increase from 11.4 kW to nearly 12.3 kW. So the most efficient condition of the turbine occur at lower temperatures. By rising the ambient temperature the exergy destruction of will increase which cause growth in overall exergy destruction while the useful exergy is constant. Therefore the abundance of the ambient temperature will reduce the total exergy.
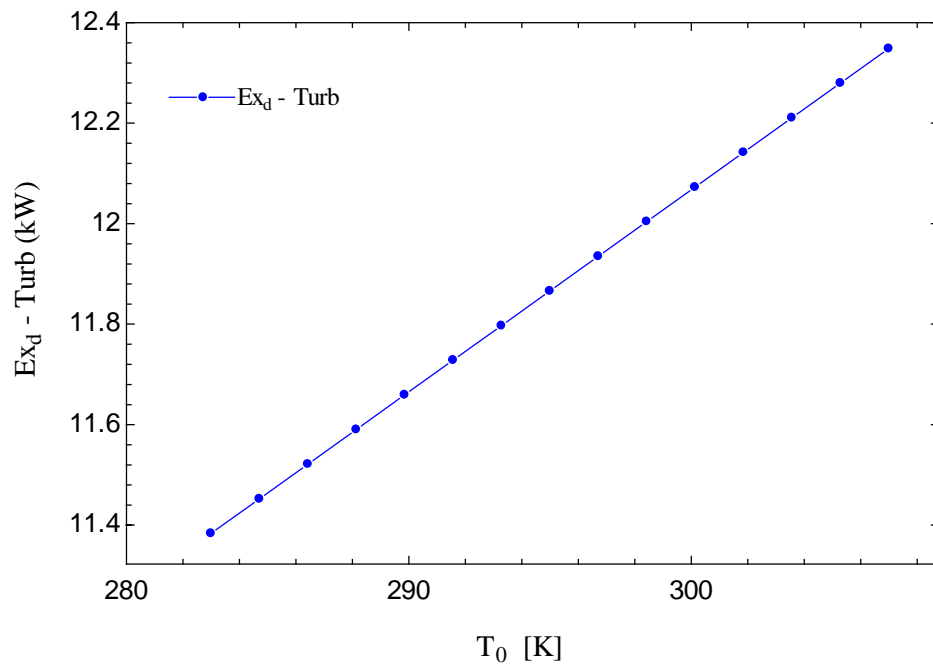
Figure 4.7: Effect of ambient temperature on exergy destruction in turbine

4.2 Analyzing the effect of inlet turbine pressure on primarily parameters

4.2.1 Analyzing the effect of inlet turbine pressure on exergy destruction of electrolyzer and turbine work

In the Figure 4.8 the relationship between inlet turbine pressures on exergy destruction of electrolyzer is presented. By rising the inlet turbine pressure from 1700 kPa to 2100 kPa, the exergy destruction of the electrolyzer will decline from 21.5 kW to nearly 19 kW. Thus the foremost performance of the electrolyzer occurs at lower pressures among 1700 kPa to 1800 kPa. Also the efficacy of the inlet turbine pressure on the total work done by the turbine is presented. As it is obvious in the figure the interval of overall work done by the turbine is from 48 to 54 kJ/kg which decrease by increasing the inlet pressure of turbine between 1700 and 2100 kPa. So the most efficient range for the turbine is between 1700 and 1800 kPa. Increasing inlet pressure reduces turbine work. From this point it is disadvantageous. However it also reduces exergy destruction in electrolyzer which is an advantageous aspect. Therefore 1700-1800 kPa range seems as optimal turbine inlet pressure.
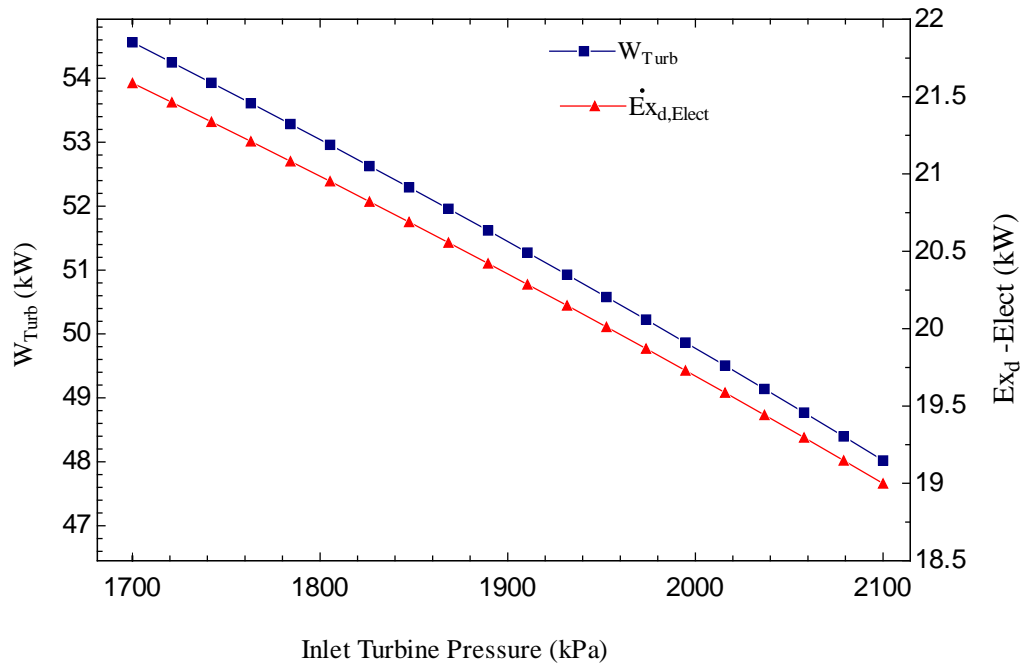
Figure 4.8: Effect of inlet turbine pressure on exergy destruction of electrolyzer and turbine work

4.2.2 Analyzing the effect of inlet turbine pressure on produced hydrogen

As shown in the Figure 4.9, by augmenting the inlet turbine pressure from 1700 kPa to 2100 kPa, the hydrogen produced in the system will decrease amongst 0.39 kg/h to nearly 0.34 kg/h. So the most efficient condition of the turbine occur at lower pressures. As the turbine inlet pressure is increased, output power by ORC turbine will growth, moreover growth in turbine work, terminates in increase in supplied electricity to the electrolyzer, then more hydrogen is produced in a same period of time.
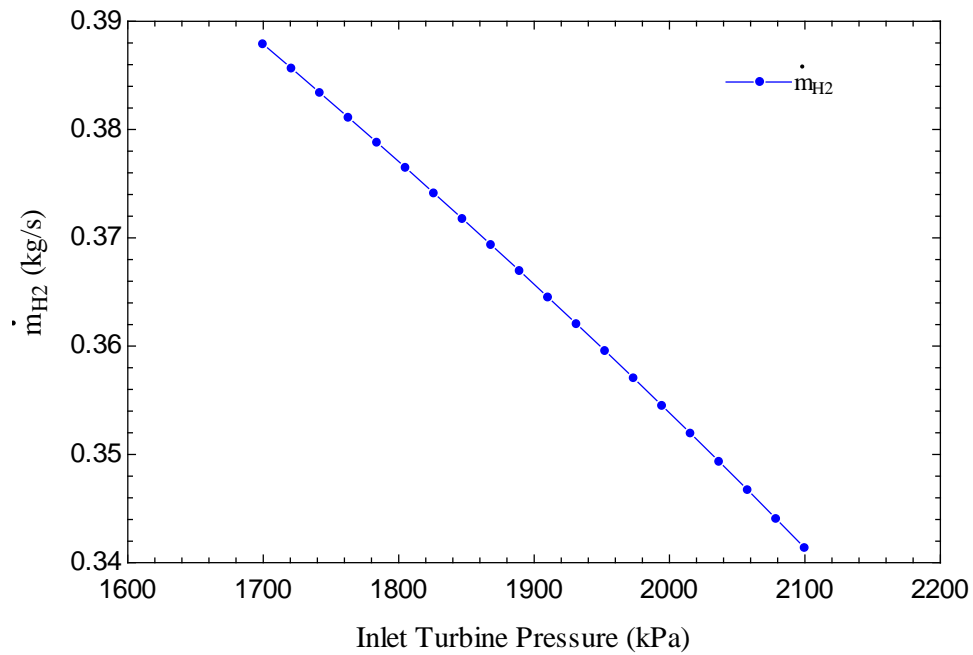
Figure 4.9: Effect of inlet turbine pressure on hydrogen produced

4.3 Analyzing the effect of ambient temperature on exergetic and energetic coefficient of performance

The Figure 4.10 represents the effect of ambient temperature on exergetic and energetic coefficient of performance of the cycle. The ambient temperature range alter across 283 K to 308 K. As it is clear, the energetic coefficient of performance is constant at 0.84 while the exergetic COP rising up from 0.1 to almost 0.9 at 308 K. Since ambient temperature does not exist in energy assessment and energy equations, the results of energetic coefficient of performance does not depends on ambient temperature, while, exergetic analysis is comprehensively up to ambient temperature and cause change in the graph. Despite increase of total exergy destruction is the reaction of the system performance for growth of ambient temperature, the overall exergy efficiency is risen up.
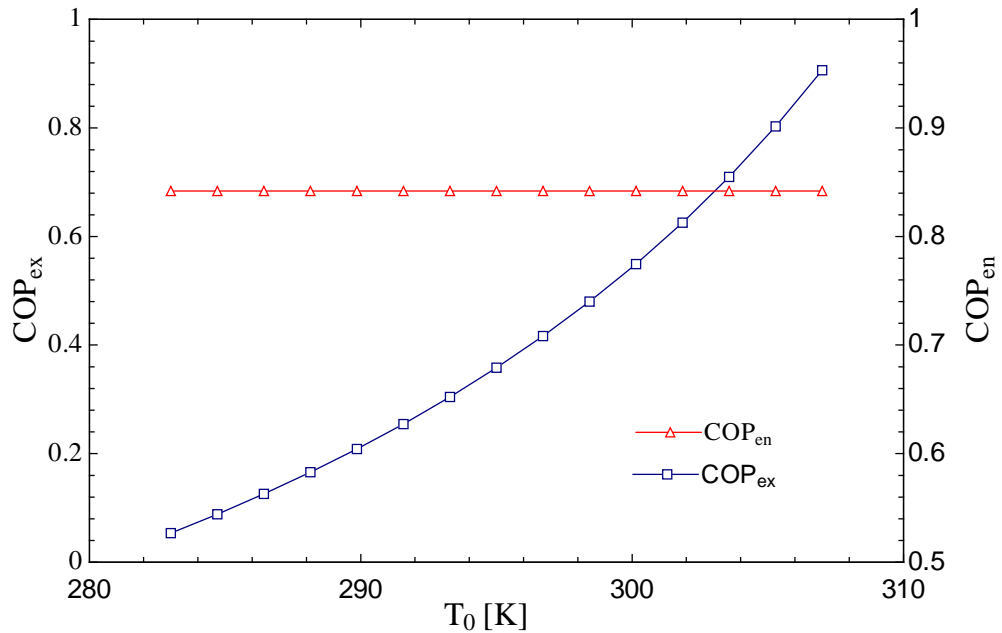
Figure 4.10: Effect of ambient temperature on exergetic and energetic coefficient of performance

4.4 Analyzing the effect of geothermal temperature and mass flow rate on exergetic and energetic primarily parameters

4.4.1 Analyzing the effect of geothermal mass flow rate on turbine work and generated hydrogen

In the Figure 4.11 the effect of geothermal mass flow rate on turbine work and generated hydrogen is illustrated. According to the diagram the turbine work period is between 0 and 96 kW while hydrogen generated rate is changing from 0 to 0.65 moreover the mass flow rate of geothermal is among 10.5 and 13 kg/s. As geothermal mass flow rate is increasing, the injected heat to the n-pentane is increased. So enthalpy of the inlet flow to turbine increases. Higher enthalpy in turbine inlet, produce more shaft work. By increasing turbine shaft work, more electricity is applied to the electrolyzer and more h_2 will produced.
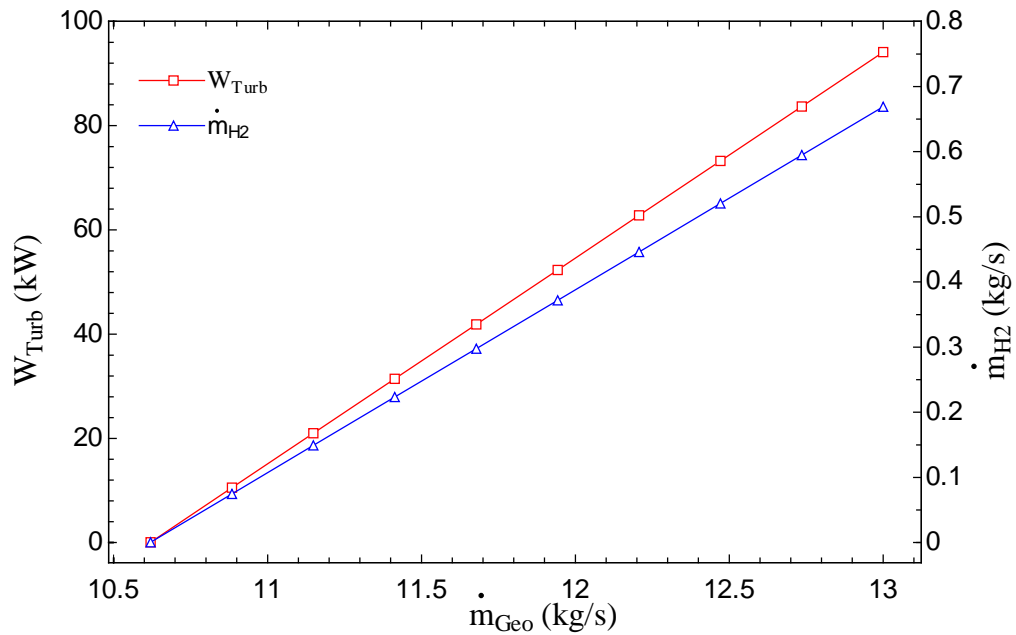
Figure 4.11: Effect of geothermal mass flow rate on turbine work and generated hydrogen

4.4.2 Analyzing the effect of geothermal mass flow rate on total exergy destruction and exergy efficiency

Based upon the Figure 4.12 the effect of geothermal mass flow rate on total exergy destruction and exergy efficiency is presented. The variation of the total exergy destruction is among 286 and 320 kW while total exergy destruction alter from 0.2 to 0.56 kW. The mass flow rate of geothermal is among 10.5 and 13 kg/s. it is expected that by increasing input heat to the system exergy destruction is increased, but this increment is not more than growth of useful exergy production by system. So exergy efficiency is rising. The geothermal temperature and mass flow rate of this assessment considered as 483.15 K and 11.88 kg/s respectively.
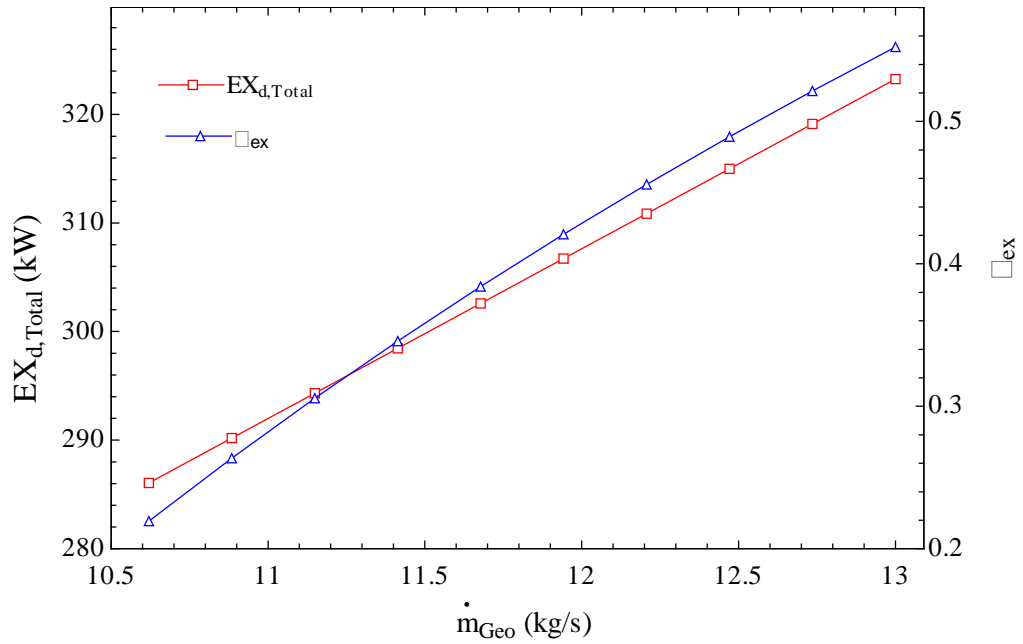
Figure 4.12: Effect of geothermal mass flow rate on total exergy destruction and exergy efficiency

4.4.3 Analyzing the effect of geothermal mass flow rate on energetic and exergetic efficiencies

In the Figure 4.13 the efficacy of the geothermal mass flow rate on the energetic and exergettic efficiencies are presented. Based on the figure the energy performance of the utility alter from 0.51 to 0.58 while the exergy efficiency changed between 0.22 and 0.55. The interval of the geothermal mass flow rate is from 10.5 to 13 kg/s. The increase in ORC turbine work is the most important reason in growth of energy efficiency. Since turbine's irreversibility is not increasing too much exergy efficiency is rising by produced exergy of turbine.
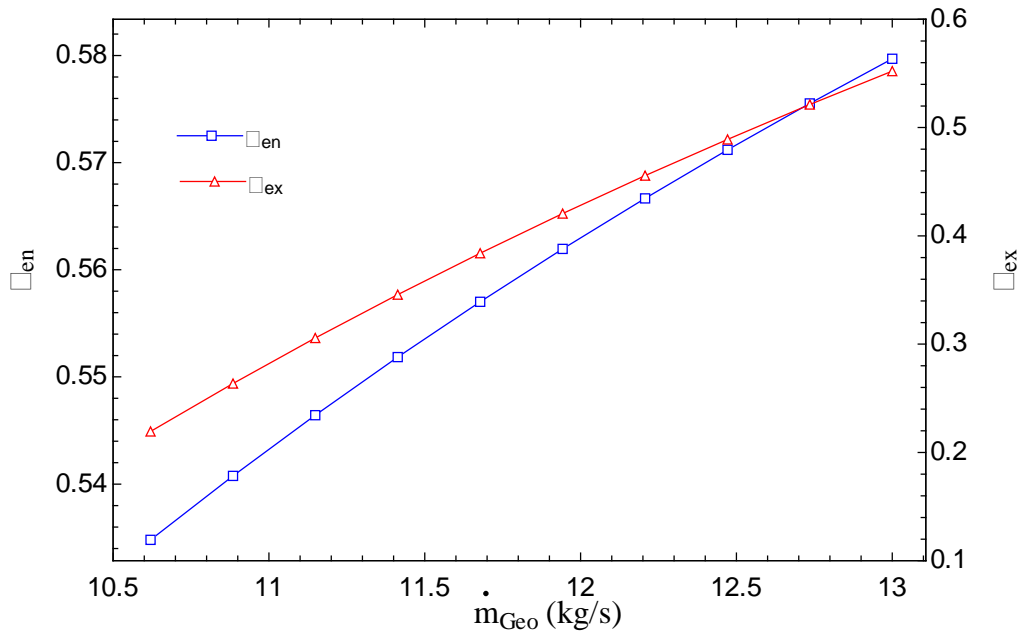
Figure 4.13: Effect of geothermal mass flow rate on energetic and exergetic efficiencies

4.4.4 Analyzing the effect of geothermal temperature on turbine work and generated hydrogen

As demonstrated in the Figure 4.14 the effect of geothermal temperature on turbine work and generated hydrogen is presented. The turbine work interval is from 49 to 74 kW. Hydrogen generated rate is altering from 0.35 to 0.53 kg/s. The variation of geothermal temperature is among 500 to 700 K. As geothermal temperature is increasing, the injected heat to the boiler increases. So enthalpy of n-pentane in inlet of turbine increases and more shaft work is produced. By increasing turbine shaft work, more electricity is applied to the electrolyzer and more H_2 will produced. Then more electricity is achieved by electrolyzer and production of hydrogen will increase.
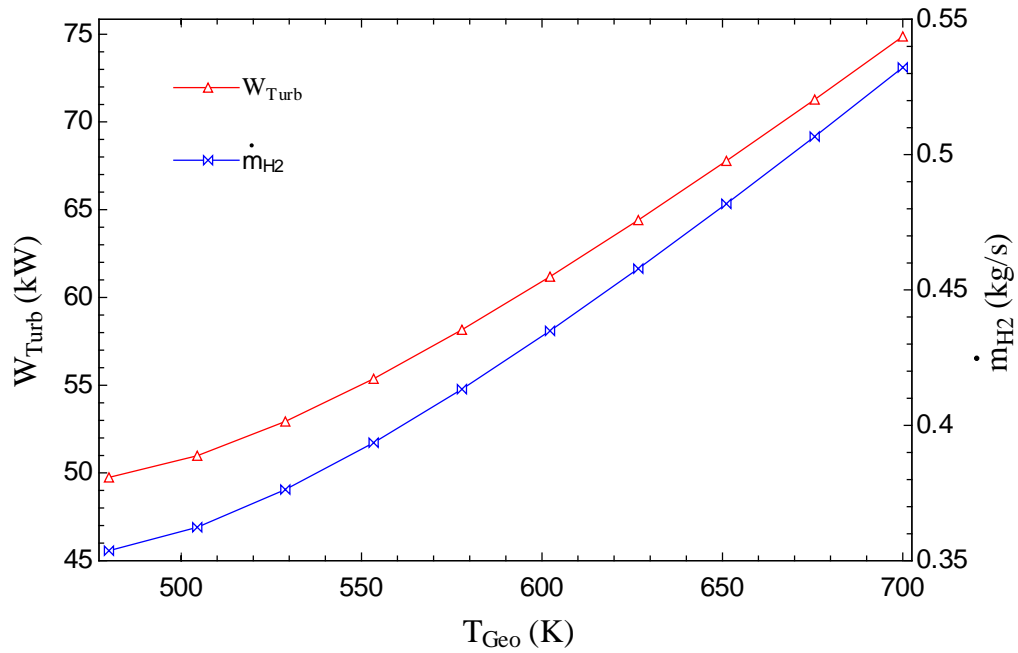
Figure 4.14: Effect of geothermal temperature on turbine work and generated hydrogen

4.4.5 Analyzing the effect of geothermal temperature on total exergy destruction and exergy efficiency

The Figure 4.15 presents the effect of geothermal temperature on total exergy destruction and exergetic efficiency of the utility. The geothermal temperature range alter across 500 K to 700 K. As it is obvious, the total exergy destruction is rising steadily from 306 to nearly 316 kW while exergetic efficiency experience a reduction from 0.41 to 0.33. Exergy destruction of boiler is get grater by entering higher temperature water to the boiler so total irreversibility increases. Since increase in produced useful exergy is lower than increase in total destruction, the exergy efficiency declines by rising geothermal temperature.
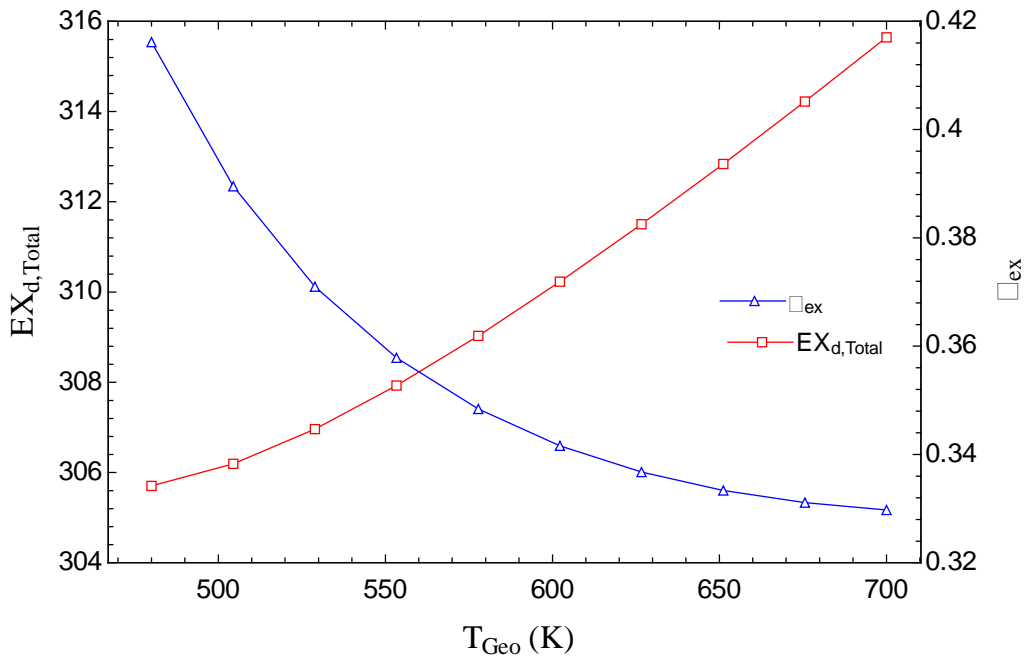
Figure 4.15: Effect of geothermal temperature on total exergy destruction and exergy efficiency

4.4.6 Analyzing the effect of geothermal temperature on energetic and exergetic efficiencies

The Figure 4.16 illustrates the effect of geothermal temperature on energetic and exergetic efficiency for this study. The geothermal temperature range changes from 480 K to 700 K. According to the graph, the energy efficiency is rising steadily from 0.561 to approximately 0.571 but exergetic efficiency experience a reduction from 0.41 to 0.33. Despite exergy efficiency declines by rising temperature because of increasing of exergy destruction, the energy efficiency is increasing, since increase in produced useful energy is more than increase in input heat to system.
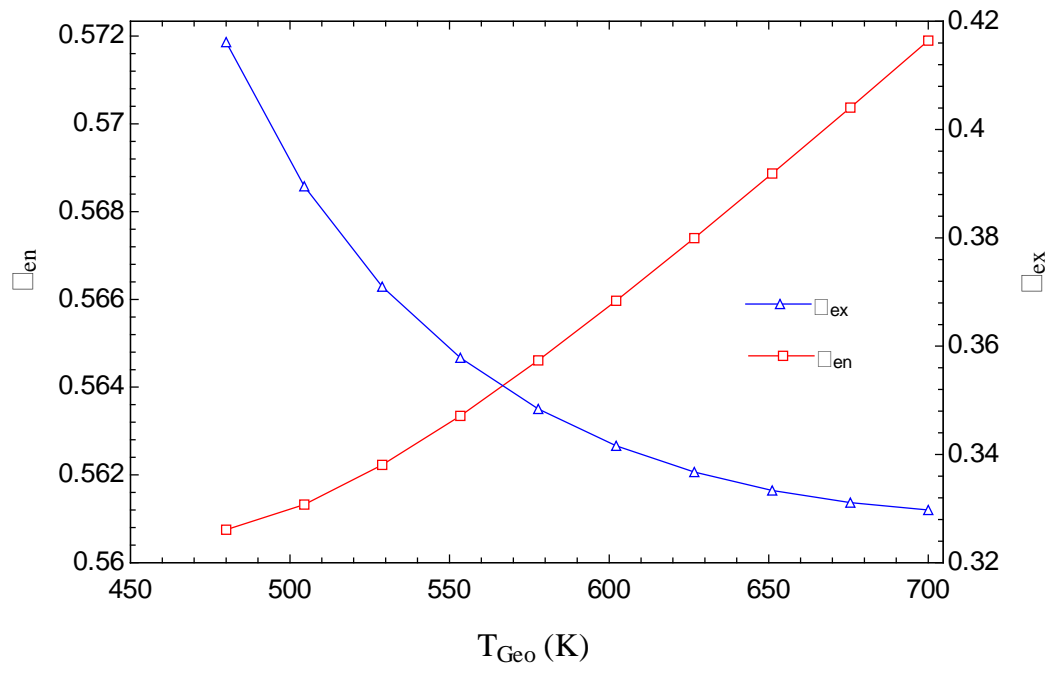
Figure 4.16: Effect of geothermal temperature on energetic and exergetic efficiencies

Chapter 5

CONCLUSION

The energetic and exergetic assessment of the multi-generation system integrated by ORC has been studied. Moreover, the effects of ambient temperature on the exergy efficacy of various parameters, the effect of inlet turbine pressure on total work of turbine, exergy destruction of electrolyzer and mass flow rate of hydrogen have been carried out.

Based on the results of this study the primarily exergy destruction takes place in boiler. Therefore, the primary causes of irreversibility are due to high inlet temperature in boiler and there is a high amount of heat transfer between geothermal hot water and n-pentane. Moreover, the inlet n-pentane fluid of boiler is saturated while the outlet phase is superheated.

According to the results achieved from this study the produced heat, produced cooling, energy spent for dehumidification, mass flow rate of hot water, mass flow rate of hydrogen and electricity produced are 248 kW, 224.3 kW, 6126 kW, 8.471 kg/s, 0.3538 kg/s and 24.98 kW respectively. Furthermore, the energy efficiency of the system is 1.59 while the exergy efficiency is about 0.4121. The COP_{en} is 0.8419 whilst the COP_{ex} is 0.4692. Finally the total exergy destruction of this utility is 305.7 kW which all these data satisfy the objectives based on (Ahmadi et al., 2011) and demonstrate that the design running properly.

REFERENCES

Ahmadi, Pouria, Dincer, Ibrahim, & Rosen, Marc A. (2011). Exergy, exergoeconomic and environmental analyses and evolutionary algorithm based multi-objective optimization of combined cycle power plants. *Energy, 36*(10), 5886-5898.

Ali, Ahmed Hamza H, Noeres, Peter, & Pollerberg, Clemens. (2008). Performance assessment of an integrated free cooling and solar powered single-effect lithium bromide-water absorption chiller. *Solar Energy, 82*(11), 1021-1030.

Andújar, José Manuel, & Segura, Francisca. (2009). Fuel cells: History and updating. A walk along two centuries. *Renewable and sustainable energy reviews, 13*(9), 2309-2322.

Angelino, G, Gaia, M, & Macchi, E. (1984). A review of Italian activity in the field of organic Rankine cycles. *VDI-Berichte*(539), 465-482.

Aphornratana, Satha, & Sriveerakul, Thanarath. (2007). Experimental studies of a single-effect absorption refrigerator using aqueous lithium–bromide: effect of operating condition to system performance. *Experimental Thermal and Fluid Science, 32*(2), 658-669.

Asghari, Saeed, Mokmeli, Ali, & Samavati, Mahrokh. (2010). Study of PEM fuel cell performance by electrochemical impedance spectroscopy. *International Journal of Hydrogen Energy, 35*(17), 9283-9290.

Athanasovici, V, Le Corre, Olivier, Brecq, G, & Tazerout, Mohand. (2000). *Thermoeconomic analysis method for cogeneration plants.* Paper presented at the OCOS 2000: FROM THERMO-ECONOMICS TO SUSTAINABILITY, PTS 1-4.

Barelli, L, Bidini, G, Gallorini, F, & Ottaviano, A. (2011). Analysis of the operating conditions influence on PEM fuel cell performances by means of a novel semi-empirical model. *international journal of hydrogen energy, 36*(16), 10434-10442.

Bereche, R Palacios, Palomino, R Gonzales, & Nebra, Silvia Azucena. (2009). Thermoeconomic analysis of a single and double-effect LiBr/H2O absorption refrigeration system. *International Journal of Thermodynamics, 12*(2), 89-96.

Bessah, R, & Benyoussef, El-Hadi. (2015). La filière des huiles essentielles Etat de l'art, impacts et enjeux socioéconomiques. *Revue des Energies Renouvelables, 18*(3), 513-528.

Borsukiewicz-Gozdur, Aleksandra, & Nowak, Władysław. (2007). Comparative analysis of natural and synthetic refrigerants in application to low temperature Clausius–Rankine cycle. *Energy, 32*(4), 344-352.

Devotta, S, & Holland, FA. (1985). Comparison of theoretical Rankine power cycle performance data for 24 working fluids. *Journal of heat recovery systems, 5*(6), 503-510.

Dickson, Mary H, & Fanelli, Mario. (2013). *Geothermal energy: utilization and technology*: Routledge.

Dincer, I, & Zamfirescu, C. (2012). Renewable-energy-based multigeneration systems. *International Journal of Energy Research, 36*(15), 1403-1415.

Dincer, Ibrahim. (2007). Environmental and sustainability aspects of hydrogen and fuel cell systems. *International Journal of Energy Research, 31*(1), 29-55.

DiPippo, Ronald. (2012). *Geothermal power plants: principles, applications, case studies and environmental impact*: Butterworth-Heinemann.

Florides, GA, Kalogirou, SA, Tassou, SA, & Wrobel, LC. (2002). Modelling and simulation of an absorption solar cooling system for Cyprus. *Solar Energy, 72*(1), 43-51.

Fridleifsson, Ingvar B. (2001). Geothermal energy for the benefit of the people. *Renewable and sustainable energy reviews, 5*(3), 299-312.

Fridleifsson, Ingvar B. (2003). Status of geothermal energy amongst the world's energy sources. *Geothermics, 32*(4), 379-388.

Gebreslassie, Berhane H, Medrano, Marc, & Boer, Dieter. (2010). Exergy analysis of multi-effect water–LiBr absorption systems: from half to triple effect. *Renewable Energy, 35*(8), 1773-1782.

Ghosh, PC, Emonts, B, Janßen, H, Mergel, J, & Stolten, D. (2003). Ten years of operational experience with a hydrogen-based renewable energy supply system. *Solar Energy, 75*(6), 469-478.

Goldemberg, Jose. (2000). *World Energy Assessment: Energy and the challenge of sustainability*: United Nations Pubns.

Harris, Daniel C. (2010). *Quantitative chemical analysis*: Macmillan.

Havelský, V. (1999). Energetic efficiency of cogeneration systems for combined heat, cold and power production. *International Journal of Refrigeration, 22*(6), 479-485.

Hollmuller, Pierre, Joubert, Jean-Marc, Lachal, Bernard, & Yvon, Klaus. (2000). Evaluation of a 5 kW p photovoltaic hydrogen production and storage installation for a residential home in Switzerland. *International Journal of Hydrogen Energy, 25*(2), 97-109.

Hovsapian, R, Vargas, JVC, Ordonez, JC, Krothapalli, A, Parise, JAR, & Berndsen, JC. (2008). Thermodynamic optimization of a solar system for cogeneration of water heating and absorption cooling. *International Journal of Energy Research, 32*(13), 1210-1227.

Izquierdo, M, Lizarte, R, Marcos, JD, & Gutiérrez, G. (2008). Air conditioning using an air-cooled single effect lithium bromide absorption chiller: results of a trial

conducted in Madrid in August 2005. *Applied Thermal Engineering, 28*(8), 1074-1081.

Jalilinasrabady, Saeid, & Itoi, Ryuichi. (2013). Classification of geothermal energy resources in Japan applying exergy concept. *International Journal of Energy Research, 37*(14), 1842-1850.

Kanoglu, Mehmet, & Bolatturk, Ali. (2008). Performance and parametric investigation of a binary geothermal power plant by exergy. *Renewable Energy, 33*(11), 2366-2374.

Khaliq, A, Kumar, R, & Dincer, I. (2009). Performance analysis of an industrial waste heat-based trigeneration system. *International journal of energy research, 33*(8), 737-744.

Kim, Byongjoo, & Park, Jongil. (2007). Dynamic simulation of a single-effect ammonia–water absorption chiller. *International Journal of Refrigeration, 30*(3), 535-545.

Liu, Bo-Tau, Chien, Kuo-Hsiang, & Wang, Chi-Chuan. (2004). Effect of working fluids on organic Rankine cycle for waste heat recovery. *Energy, 29*(8), 1207-1217.

Lund, John W, Freeston, Derek H, & Boyd, Tonya L. (2011). Direct utilization of geothermal energy 2010 worldwide review. *Geothermics, 40*(3), 159-180.

Maizza, V, & Maizza, A. (2001). Unconventional working fluids in organic Rankine-cycles for waste energy recovery systems. *Applied thermal engineering, 21*(3), 381-390.

Murphy, Hugh, & Niitsuma, Hiroaki. (1999). Strategies for compensating for higher costs of geothermal electricity with environmental benefits. *Geothermics, 28*(6), 693-711.

Ni, Meng, Leung, Michael KH, & Leung, Dennis YC. (2007). Parametric study of solid oxide fuel cell performance. *Energy Conversion and Management, 48*(5), 1525-1535.

Niksiar, Arezou, & Rahimi, Amir. (2009). Energy and exergy analysis for cocurrent gas spray cooling systems based on the results of mathematical modeling and simulation. *Energy, 34*(1), 14-21.

Ott, Wayne R. (1994). *Environmental statistics and data analysis*: CRC Press.

Ozgener, Leyla, Hepbasli, Arif, & Dincer, Ibrahim. (2005). Energy and exergy analysis of Salihli geothermal district heating system in Manisa, Turkey. *International Journal of Energy Research, 29*(5), 393-408.

Panwar, NL. (2007). *Renewable energy sources for sustainable development*: New India Publishing.

Secretariat, United Nations Environment Programme. Ozone. (2006). *Handbook for the Montreal protocol on substances that deplete the ozone layer*: UNEP/Earthprint.

Şencan, Arzu, Yakut, Kemal A, & Kalogirou, Soteris A. (2005). Exergy analysis of lithium bromide/water absorption systems. *Renewable energy, 30*(5), 645-657.

Stojić, Dragica Lj, Marčeta, Milica P, Sovilj, Sofija P, & Miljanić, Šćepan S. (2003). Hydrogen generation from water electrolysis—possibilities of energy saving. *Journal of Power Sources, 118*(1), 315-319.

Tchanche, BF, Lambrinos, Gr, Frangoudakis, A, & Papadakis, G. (2010). Exergy analysis of micro-organic Rankine power cycles for a small scale solar driven reverse osmosis desalination system. *Applied Energy, 87*(4), 1295-1306.

Ward, DS, Löf, GOG, & Uesaki, T. (1978). Cooling subsystem design in CSU solar house III. *Solar Energy, 20*(2), 119-126.

Yilanci, A, Dincer, I, & Ozturk, HK. (2008). Performance analysis of a PEM fuel cell unit in a solar–hydrogen system. *International Journal of Hydrogen Energy, 33*(24), 7538-7552.

Yilanci, A, Dincer, I, & Ozturk, HK. (2009). A review on solar-hydrogen/fuel cell hybrid energy systems for stationary applications. *Progress in Energy and Combustion Science, 35*(3), 231-244.

Zeng, Kai, & Zhang, Dongke. (2010). Recent progress in alkaline water electrolysis for hydrogen production and applications. *Progress in Energy and Combustion Science, 36*(3), 307-326.

APPENDICES

Appendix A: Engineering Equation Solver Codes

"surrounding states"

t[0]=25+273.15

h[0]=Enthalpy(air,T=T[0])

s[0]=Entropy(air,T=T[0],P=P[0])

p[0]=100

ex[0]=((h[0]-h[0])-t[0]*(s[0]-s[0]))

m_dot[1]=11.88

p[1]=100

t[1]=210+273.15

h[1]=Enthalpy(Water,t=t[1],P=P[2])

s[1]=Entropy(Water,T=T[1],P=P[1])

ex[1]=(h[1]-h[0])-t[0]*(s[1]-s[0])

m_dot[2]=m_dot[1]

p[2]=p[1]

t[2]=t[1]-20

h[2]=Enthalpy(Water,t=t[2],P=P[2])

s[2]=Entropy(Water,T=T[2],P=P[2])

ex[2]=(h[2]-h[0])-t[0]*(s[2]-s[0])

"n-nonane Turbine"

Q_h=m_dot[1]*(h[1]-h[2])

Q_h=m_dot[3]*(h[3]-h[17])

ex_boiler=Q_h*(1-t[0]/t[3])

m_dot[3]=0.498

p[3]=2000

t[3]=465

"h[3]=Enthalpy(n-Pentane,T=T[3],P=P[3])"

s[3]=Entropy(n-Pentane,T=T[3],P=P[3])

ex[3]=((h[3]-h[0])-t[0]*(s[3]-s[0]))

m_dot[4]=m_dot[3]

p[4]=100

t[4]=400

h[4]=Enthalpy(n-Pentane,T=T[4],P=P[4])

s[4]=Entropy(n-Pentane,T=T[4],P=P[4])

ex[4]=((h[4]-h[0])-t[0]*(s[4]-s[0]))

w_dotT=m_dot[3]*(h[3]-h[4])

ex_dotdesT+m_dot[4]*ex[4]+w_dotT=m_dot[3]*ex[3]

61

m_dot[5]=m_dot[4]

p[5]=p[4]

t[5]=Temperature(n-Pentane,P=P[5],h=h[5])

x[5]=Quality(n-Pentane,T=T[5],h=h[5])

s[5]=Entropy(n-Pentane,x=x[5],P=P[5])

ex[5]=((h[5]-h[0])-t[0]*(s[5]-s[0]))

m_dot[6]=m_dot[5]

p[6]=p[5]

t[6]=Temperature(n-Pentane,P=P[6],x=x[6])

x[6]=0

h[6]=Enthalpy(n-Pentane,x=x[6],P=P[6])

s[6]=Entropy(n-Pentane,x=x[6],P=P[6])

ex[6]=((h[6]-h[0])-t[0]*(s[6]-s[0]))

m_dot[4]*h[4]+m_dot[9]*h[9]=m_dot[10]*h[10]+m_dot[13]*h[13]+m_dot[5]*h[5]

m_dot[4]*ex[4]+((tG-t[0])/tG)*q_dotG=m_dot[5]*ex[5]+ex_des_Boi

m_dot[17]=m_dot[6]

p[17]=p[3]

t[17]=t[6]

h[17]=Enthalpy(n-Nonane,t=t[17],P=P[17])

s[17]=Entropy(n-Nonane,t=t[17],P=P[17])

ex[17]=((h[17]-h[0])-t[0]*(s[6]-s[0]))

v[17]=Volume(n-Nonane,T=T[17],P=P[17])

"pump2"

w_dotP2=m_dot[6]*(v[17]*(p[17]-p[6]))

m_dot[6]*ex[6]+w_dotP2=m_dot[17]*ex[17]+ex_dotdesP2

"j"

m_dot[7]=1.145

x[7]=0.5225

p[7]=1

t[7]=32+273.15

s[7]=s_LiBrH2O(T[7],x[7])

h[7]=h_LiBrH2O(T[7],x[7])

ex[7]=((h[7]-h[0])-t[0]*(s[7]-s[0]))

v[7]=1/rho_LiBrH2O(T[7],X[7])

m_dot[8]=m_dot[7]

x[8]=x[7]

p[8]=4.81

t[8]=t[7]

s[8]=s_LiBrH2O(T[8],x[8])

h[8]=h_LiBrH2O(T[8],x[8])

ex[8]=((h[8]-h[0])-t[0]*(s[8]-s[0]))

w_dotp3=m_dot[8]*v[7]*(p[8]-p[7])

w_dotp3+m_dot[7]*ex[7]=m_dot[8]*ex[8]+ex_dotdesp3

m_dot[9]=m_dot[7]

x[9]=x[7]

t[9]=57.9+273.15

p[9]=p[8]

{h[9]=h_LiBrH2O(t[9];x[9])}

s[9]=s_LiBrH2O(t[9],x[9])

ex[9]=((h[9]-h[0])-t[0]*(s[9]-s[0]))

(m_dot[10]*h[10]-m_dot[11]*h[11])*0.9=(m_dot[9]*h[9]-m_dot[8]*h[8])

m_dot[10]*x[10]=m_dot[9]*x[9]

x[10]=0.5694

t[10]=69.8+273.15

p[10]=p[8]

h[10]=h_LiBrH2O(T[10],x[10])

s[10]=s_LiBrH2O(t[10],x[10])

ex[10]=((h[10]-h[0])-t[0]*(s[10]-s[0]))

m_dot[11]=m_dot[10]

x[11]=x[10]

p[11]=p[8]

t[11]=32.2+273.15

h[11]=h_LiBrH2O(T[11],x[11])

s[11]=s_LiBrH2O(T[11],x[11])

ex[11]=((h[11]-h[0])-t[0]*(s[11]-s[0]))

m_dot[12]=m_dot[10]

x[12]=x[10]

t[12]=32.2+273.15

p[12]=p[7]

h[12]=h_LiBrH2O(T[12],x[12])

s[12]=s_LiBrH2O(t[12],x[12])

ex[12]=((h[12]-h[0])-t[0]*(s[12]-s[0]))

m_dot[13]=m_dot[9]-m_dot[10]

p[13]=p[10]

t[13]=67+273.15

h[13]=Enthalpy(Water,T=T[13],P=P[13])

s[13]=Entropy(Water,T=T[13],P=P[13])

ex[13]=((h[13]-h[0])-t[0]*(s[13]-s[0]))

m_dot[14]=m_dot[13]

p[14]=p[13]

t[14]=32.19+273.15

h[14]=Enthalpy(Water,T=T[14],P=P[14])

s[14]=Entropy(Water,T=T[14],P=P[14])

ex[14]=((h[14]-h[0])-t[0]*(s[14]-s[0]))

m_dot[15]=m_dot[13]

p[15]=p[7]

x[15]=Quality(Water,T=T[15],h=h[15])

t[15]=7+273.15

h[15]=h[14]

s[15]=Entropy(Water,x=x[15],t=t[15])

ex[15]=((h[15]-h[0])-t[0]*(s[15]-s[0]))

m_dot[16]=m_dot[13]

p[16]=p[15]

x[16]=1

t[16]=7+273.15

h[16]=Enthalpy(Water,x=x[16],P=P[16])

s[16]=Entropy(Water,p=p[16],t=t[16])

ex[16]=((h[16]-h[0])-t[0]*(s[16]-s[0]))

{m_dot[18]}

p[18]=100

t[18]=t[0]

h[18]=Enthalpy(Water,t=t[18],P=P[18])

s[18]=Entropy(Water,t=t[18],P=P[18])

ex[18]=((h[18]-h[0])-t[0]*(s[18]-s[0]))

m_dot[19]=m_dot[18]

p[19]=100

t[19]=t[7]

h[19]=Enthalpy(Water,T=T[19],P=P[19])

s[19]=Entropy(Water,T=T[19],P=P[19])

ex[19]=((h[19]-h[0])-t[0]*(s[19]-s[0]))

q_dotG+m_dot[9]*h[9]=m_dot[10]*h[10]+m_dot[13]*h[13]

ex_dotG=((tG-t[0])/tG)*q_dotG

tG=(t[10]+t[9])/2

q_dotCond=m_dot[13]*h[13]-m_dot[14]*h[14]

ex_dotCond+m_dot[13]*ex[13]=Des_dotCond+m_dot[14]*ex[14]

ex_dotCond=((tCond-t[0])/tCond)*q_dotCond

tCond=(t[14]+t[13])/2

COP_en=q_dotEva/(q_dotG+w_dotp3)

COP_ex=ex_dotEva/(ex_dotG+w_dotp3)

q_dotEva=m_dot[16]*(h[16]-h[15])

ex_dotEva=((t[0]-tEva)/tEva)*q_dotEva

(t[15]+t[16])/2=tEva

q_dotAbs=m_dot[19]*h[19]-m_dot[18]*h[18]

ex_q_dotAbs=m_dot[19]*ex[19]-m_dot[18]*ex[18]

q_dotAbs=m_dot[16]*h[16]+m_dot[12]*h[12]-m_dot[7]*h[7]

m_dot[16]*ex[16]+m_dot[12]*ex[12]+m_dot[18]*ex[18]=Des_dotabs+m_dot[7]*ex[7]+m_dot[19]*ex[19]

{m_dot[20]=}

t[20]=t[0]

p[20]=p[0]

rh[20]=0.8

h[20]=Enthalpy(AirH2O,T=T[20],r=rh[20],P=P[20])

s[20]=Entropy(AirH2O,T=T[20],r=rh[20],P=P[20])

ex[20]=((h[20]-h[0])-t[0]*(s[20]-s[0]))

omega[20]=HumRat(AirH2O,T=T[20],r=rh[20],P=P[20])

m_dot[21]=m_dot[20]

t[21]=t[0]-4

p[21]=p[0]

rh[21]=1

h[21]=Enthalpy(AirH2O,T=T[21],r=rh[21],P=P[21])

s[21]=Entropy(AirH2O,T=T[21],r=rh[21],P=P[21])

ex[21]=((h[21]-h[0])-t[0]*(s[21]-s[0]))

omega[21]=HumRat(AirH2O,T=T[21],r=rh[21],P=P[21])

p[22]=p[20]

t[22]=t[21]

h[22]=Enthalpy(Water,T=T[22],P=P[22])

s[22]=Entropy(Water,T=T[22],P=P[22])

ex[22]=((h[22]-h[0])-t[0]*(s[22]-s[0]))

q_dotoutdryer=q_dotEva

m_dot[20]*omega[20]=m_dot[21]*omega[21]+m_dot[22]

m_dot[20]*h[20]=q_dotoutdryer+m_dot[21]*h[21]+m_dot[22]*h[22]

m_dot[20]*ex[20]+ex_dotdesDryer=m_dot[21]*ex[21]+m_dot[22]*ex[22]+ex_dotE

(m_dot[24]*exchemH2O)+m_dot[24]*ex[24]+etaelectrolyzer*w_dotT=m_dot[23]*exchemH2+m_dot[23]*ex[23]+m_dot[25]*ex[25]+m_dot[25]*exchemO2+ex_dotdesElectrolyzer

etaelectrolyzer=0.56

W_lossElectrolyzer=(1-etaelectrolyzer)*(1*w_dotT)

HHV=141800

MH2=MolarMass(H2)

m_dot[23]=(etaelectrolyzer*w_dotT*0.5)/HHV

p[23]=100

t[23]=60+273.15

h[23]=Enthalpy(H2,T=T[23])

s[23]=Entropy(H2,T=T[23],P=P[23])

ex[23]=((h[23]-h[0])-t[0]*(s[23]-s[0]))

exchemH2=(236.09*1000)/MH2

exchemH2*m_dot[23]=ex_doth2

MO2=MolarMass(O2)

m_dot[25]=(m_dot[23]/MH2)*(0.5)*MO2

p[25]=100

t[25]=60+273.15

h[25]=Enthalpy(O2,T=T[25])

s[25]=Entropy(O2,T=T[25],P=P[25])

ex[25]=((h[25]-h[0])-t[0]*(s[25]-s[0]))

exchemO2=(3.97*1000)/MO2

MH2O=MolarMass(Water)

m_dot[24]=(m_dot[23]/MH2)*MH2O

t[24]=25+273.15

p[24]=100

h[24]=Enthalpy(Water,T=T[24],P=p[24])

s[24]=Entropy(Water,T=T[24],P=P[24])

ex[24]=((h[24]-h[0])-t[0]*(s[24]-s[0]))

exchemH2O=(0.9*1000)/MH2O

m_dotwater=m_dot[24]*3.600

m_dotH2=m_dot[23]*3600

exH2=m_dot[23]*HHV

ex_input=Q_h*(1-t[0]/t[1])

Electricite=w_dotT*0.5

Eta_en=(m_dot[23]*HHV+q_dotEva+Electricite+q_dotAbs+q_dotCond)/Q_h

Eta_ex=(ex_dotCond+exH2+ex_dotEva+ex_q_dotAbs+Electricite)/ex_input

Q_dot_heating=m_dot[18]*(h[19]-h[18])

m_dot[21]*(h[19])=Dehumidifing_energy

des_dottotal=ex_dotdesT+ex_des_Boi+ex_dotdesP2+ex_dotdesp3+Des_dotCond+D

es_dotabs+ex_dotdesDryer+ex_dotdesElectrolyzer

Appendix B: Chemical Exergy of Various Substances

Element	Chemical Exergy[kJ/kmol]
C(solid)	410 260
H2	236 090
CO	275 075
CO2	19 850
H2O (liquid)	0
H2O (vapor)	9 845
CH4	831 720
N2	720
O2	3 970